Computational Teleology in Holographic Polar Arithmetic: Scan Complexity, Readout Resolution, and an Undecidable Quantum-Cellular Universe

Haobo Ma*
AELF PTE LTD.
#14-02, Marina Bay Financial Centre Tower 1, 8 Marina Blvd, Singapore 018981

January 1, 2026

Abstract

We develop an operational isomorphism between *complexity*, *geometry*, and *observation* within a unified syntax for Holographic Polar Arithmetic (HPA) and Omega Theory. In this framework, computational resources are not external bookkeeping but internal geometric costs of a scan–readout protocol: time is defined as the iteration count of a genuine unitary scan operator Θ, while space is defined as readout resolution (prefix length and orthogonal cut capacity) induced by a window projection Π_W and its canonical coding (Ostrowski numeration, specializing to Zeckendorf in the golden branch). The scan shift and phase multiplication form a Weyl pair, yielding a variance-type uncertainty relation that forbids simultaneous minimization of scan-localization and readout-localization, thereby providing a structural time–space complementarity.

On the dynamical side, Omega Theory models microscopic evolution as a partitioned quantum cellular automaton (PQCA) and supports an *exact* compilation of a local PQCA step on a finite region into a one-dimensional nearest-neighbor circuit. The resulting compilation depth defines a routing overhead κ and an emergent computational lapse field $\mathcal{N}(x) = \kappa_0/\kappa(x)$, making gravitational time dilation equivalent to computational slowdown in an operational sense (Appendix F). At the computability layer, universal QCA dynamics admits an undecidable local reachability predicate by reduction from reversible halting (Appendix G), which provides a theorem-level "open-endedness boundary" for prediction.

We emphasize a strict separation of layers: undecidability is a theorem about internal predicates, whereas modeling observers as interactive machines with oracle-like interfaces is an *interpretation-layer* language for resource injection and conditionalization, not a deduction about physical collapse. Finally, the discrete scan provides an exact lattice dispersion relation whose low-energy limit recovers approximately linear propagation and whose high-energy deviation yields a testable template for energy-dependent corrections to effective signal speed.

Keywords: Holographic Polar Arithmetic; Omega Theory; quantum cellular automata; time complexity; space complexity; Weyl pair; Ostrowski numeration; Zeckendorf decomposition; undecidability; interactive computation; oracle.

Conventions. Unless otherwise stated, log denotes the natural logarithm. "mod 1" refers to reduction in $\mathbb{R}/\mathbb{Z}$, and "mod 2π" refers to reduction in $\mathbb{R}/2\pi\mathbb{Z}$.

Contents

*Email: auric@aelf.io

1 Introduction: from coordinate schematics to computational teleology

1.1 If the universe were fully decidable, why has it not "halted"?

A standard division of labor treats time as a physical parameter (or a coordinate on a background geometry) and treats time complexity as a computational resource (step count in an abstract machine). The HPA–Ω stance is more aggressive and more unified: *time and space are not background containers but internal costs paid by a readout protocol that accesses, cuts, and encodes a conserved whole.*

The motivating question can be phrased without metaphysics. If microscopic dynamics is strictly local and unitary—as in a quantum cellular automaton (QCA)—then "history" is a reversible computation. If, in addition, the internal reachability of certain local predicates is undecidable (as in universal QCAs; Appendix G), then there is no general algorithm deciding whether a given local event will ever occur from the finite description of the initial encoding. In such a setting, "the universe computing an ultimate answer and stopping" is not the generic computational narrative; undecidable reachability provides a theorem-level boundary condition for long-time prediction.

1.2 What this paper does

This paper presents a self-contained system-architecture layer for Holographic Polar Arithmetic (HPA) and Omega Theory. We treat their primitives as an axiomatic toolbox, but every theorem-level statement used in the main chain is either proved in this manuscript (often in the appendices) or cited to standard literature.

Contribution 1 (unified resource semantics). We define time complexity as scan depth (iteration count of a unitary scan Θ) and as compilation depth (1D nearest-neighbor circuit depth for implementing a local PQCA step). We define space complexity as readout resolution: prefix length of a window projection bitstream, canonical coding length (Ostrowski/Zeckendorf), and active Hilbert-workspace capacity.

Contribution 2 (hard resource complementarity). From the Weyl-pair structure $UV = \mathrm{e}^{\mathrm{i}\Phi}VU$ (scan shift vs phase) we obtain a variance-type uncertainty relation, which becomes a quantitative statement that one cannot simultaneously minimize scan-localization and readout-localization. This is the formal core behind time–space tradeoffs in the scan–readout setting. Appendix B further gives an operational form in terms of Helstrom-optimal hypothesis testing and an explicit sample-complexity lower bound for detecting a scan shift at error tolerance ϵ.

Contribution 3 (universe–QCA–undecidability chain). Omega Theory models microscopic dynamics as a PQCA, and provides an exact compilation of finite-region steps to 1D nearest-neighbor circuits. Universal QCAs support an undecidable local reachability predicate (encoding halting into a local flag). Hence, in the "universe as computation" model, open-endedness is a theorem-level boundary condition rather than a purely philosophical slogan.

Contribution 4 (observer as an interactive interface; interpretation layer). We model an observer as an interactive machine that continually exchanges information with the environment. Treating "selection" or "collapse" as an oracle-like resource input is an *interpretation-layer* language for conditionalization on undecidable predicates; it is not a physical conclusion forced by the undecidability theorem.

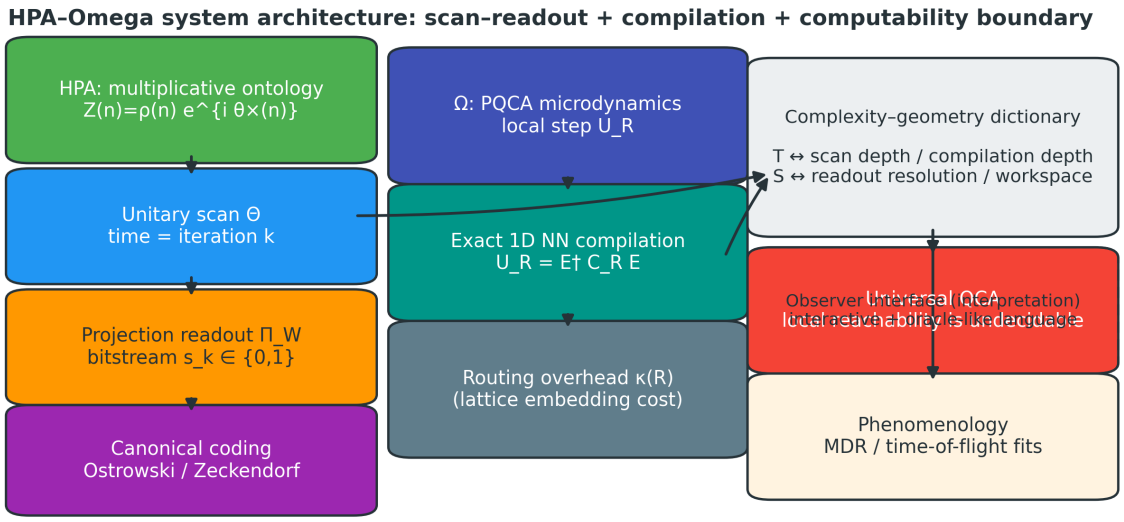

Figure 1: **HPA–Ω system architecture.** The paper organizes three layers: (i) a formal operator/coding layer (scan and readout), (ii) a computational implementation layer (1D compilation and routing overhead), and (iii) a computability boundary layer (undecidable reachability), with a strict separation between theorem statements and interpretation-layer mappings.

Contribution 5 (a testable dispersion template). The discrete scan yields an exact lattice dispersion relation whose low-energy limit is approximately linear. The high-energy deviation provides a concrete template for energy-dependent corrections to effective propagation speed.

1.3 Logic audit: definition edges, theorem edges, interpretation edges

To keep the chain explicit, we distinguish three edge types.

- **Definition edge**: an internal definition within the HPA–Ω formalism.
- **Theorem edge**: a mathematical statement proved in this manuscript or cited to standard literature.
- **Interpretation edge**: a mapping from formal objects to physical language; this is not a theorem and must remain clearly marked.

The main chain of this paper is summarized in Table 1.

2 Formal interface: HPA and Omega Theory in one syntax

2.1 HPA: multiplicative ontology, scan time, and projection readout

We adopt the multiplicative-first stance: multiplication is treated as primitive structure, while classical linear addition is realized operationally as a (lossy) readout. The starting point is the multiplicative skeleton

$$M = (\mathbb{N}_{>0}, \cdot), \tag{1}$$

augmented by a radial character $\rho : M \to \mathbb{R}_{>0}$ and a multiplicative phase $\theta_\times : M \to \mathbb{R}/2\pi\mathbb{Z}$ that is additive under multiplication. The basic embedding is

$$\mathcal{Z}(n) = \rho(n)\mathrm{e}^{\mathrm{i}\theta_\times(n)} \in \mathbb{C}^*, \qquad \mathcal{Z}(mn) = \mathcal{Z}(m)\mathcal{Z}(n). \tag{2}$$

Edge	Claim / link in the chain
Def.	HPA defines a multiplicative polar embedding $\mathcal{Z}(n) = \rho(n)\mathrm{e}^{\mathrm{i}\theta_\times(n)}$ and introduces a genuine unitary scan operator Θ, defining time as iteration count.
Thm.	No-go: a map $\Phi : \mathbb{N}_{>0} \to \mathbb{C}$ cannot be simultaneously multiplicative and linearly additive except in the trivial/identity cases (Theorem 2.3); therefore addition must be realized as a lossy readout/projection, producing a structural gap.
Def.	Window projection Π_W produces a binary mechanical word; the golden branch selects Zeckendorf/Ostrowski canonical coding.
Thm.	The scan shift and phase operator form a Weyl pair and satisfy an uncertainty relation, yielding a hard time–space complementarity; operationally this can be phrased as a hypothesis-testing and sample-complexity tradeoff (Appendix B).
Def.	Omega Theory models microdynamics as a PQCA; a local step on a finite region is exactly compilable to a 1D nearest-neighbor circuit. Compilation depth defines routing overhead κ and lapse $\mathcal{N} = \kappa_0/\kappa$.
Thm.	In a universal QCA, a local reachability predicate can encode reversible halting and is undecidable.
Interp.	An observer is modeled as an interactive machine; "selection" can be spoken of as oracle-like resource input for conditioning on undecidable predicates (a language choice, not a physical theorem).
Model	Discrete scan induces an exact dispersion relation with low-energy linearity and high-energy deviations, providing a testable template for effective signal-speed corrections.

Table 1: **Logic chain audit.** Definition edges are internal to the formalism; theorem edges are mathematical statements; interpretation edges are semantic mappings that must remain clearly separated.

Remark 2.1 (Explicit parametrization via prime data)**.** *Writing $n = \prod_p p^{v_p(n)}$, any choice of prime parameters (r_p, ϑ_p) with $r_p > 0$ and $\vartheta_p \in \mathbb{R}/2\pi\mathbb{Z}$ induces*

$$\rho(n) := \prod_p r_p^{v_p(n)}, \qquad \theta_\times(n) := \sum_p v_p(n)\,\vartheta_p \pmod{2\pi}, \tag{3}$$

and hence $\mathcal{Z}(n) = \prod_p (r_p \mathrm{e}^{\mathrm{i}\vartheta_p})^{v_p(n)}$ is multiplicative. This makes explicit that the embedding is fully determined by its values on primes.

Remark 2.2 (What depends on $\mathcal{Z}$ in this manuscript)**.** *All theorem-level results used in the main chain (discrepancy/readout scaling, Weyl-pair complementarity, compilation-overhead bounds, undecidable reachability, and the dispersion template) do not require any further specification of the prime parameters beyond multiplicativity. The embedding $\mathcal{Z}$ enters only when one chooses a concrete additive readout rule R (Remark 2.5) and studies embedding-dependent quantities such as the quantum gap (Definition 2.4).*

To decouple intrinsic phase from readout order, HPA introduces a *genuine* unitary scan operator Θ and defines time as iteration count $k \in \mathbb{Z}_{\geq 0}$. In the minimal model, Θ may be realized as a Koopman shift for an irrational rotation on $L^2(S^1)$,

$$(\Theta f)(x) = f(x + \alpha), \qquad \alpha \in \mathbb{R} \setminus \mathbb{Q}. \tag{4}$$

Here we take $S^1 = \mathbb{R}/\mathbb{Z}$ with coordinate $x \in [0, 1)$ and Haar measure dx. Fix a measurable window $W \subset S^1$ and let $\chi_W : S^1 \to \{0, 1\}$ denote its indicator. The corresponding sharp window projection is the multiplication operator

$$(\Pi_W f)(x) := \chi_W(x)\, f(x), \qquad \Pi_W^2 = \Pi_W = \Pi_W^\dagger. \tag{5}$$

In the classical orbit limit (a sharply localized phase x_0), readout produces the mechanical/Sturmian word

$$s_k := \chi_W(x_0 + k\alpha) \in \{0, 1\}. \tag{6}$$

For interval windows, this is the standard Sturmian construction; in particular, the prefix sums satisfy the exact discrepancy identity

$$S_N := \sum_{k=0}^{N-1} s_k = \lfloor N\alpha + \beta \rfloor - \lfloor \beta \rfloor \tag{7}$$

for a phase offset β determined by x_0 and the window convention [1, 2].

Readout as a two-outcome measurement/instrument. At the interface layer, the same window cut can be expressed as a standard two-outcome quantum measurement [3]. The sharp readout is the projective measurement (PVM) $\{\Pi_W,\ \mathbb{1} - \Pi_W\}$ on $L^2(S^1)$. Given a state ρ, the Born probability for outcome "1" is $p_1 = \mathrm{Tr}(\Pi_W \rho)$, and the associated Lüders instrument maps

$$\rho \longmapsto \frac{\Pi_W \rho\, \Pi_W}{\mathrm{Tr}(\Pi_W \rho)} \qquad \text{or} \qquad \rho \longmapsto \frac{(\mathbb{1} - \Pi_W)\rho\,(\mathbb{1} - \Pi_W)}{\mathrm{Tr}((\mathbb{1} - \Pi_W)\rho)}, \tag{8}$$

conditioned on the respective outcomes. If one samples after k scan steps, $\rho_k = \Theta^k \rho_0 \Theta^{-k}$ and $p_k = \mathrm{Tr}(\Pi_W \rho_k)$. In the idealized phase-eigenstate limit $|x_0\rangle$ (or a narrow wavepacket around x_0), this reduces to the deterministic orbit rule $p_k = \chi_W(x_0 + k\alpha)$ in (6).
More realistic readouts are naturally modeled by POVMs: for a "soft window" $w : S^1 \to [0, 1]$, define commuting Kraus operators $M_1 f = \sqrt{w}\, f$ and $M_0 f = \sqrt{1 - w}\, f$, yielding effects $E_1 = M_1^\dagger M_1$ and $E_0 = M_0^\dagger M_0$ with $E_0 + E_1 = \mathbb{1}$. This makes explicit how Π_W is the sharp ($w = \chi_W$) limit of a standard instrument model.
Within a QCA substrate, such readouts can be realized by a standard dilation: any POVM can be implemented by coupling the system locally to an ancilla via a unitary and then performing a projective measurement on the ancilla (Naimark/Stinespring-type realizations; see, e.g., [3,4]). This places Π_W and its noisy variants within the usual local-unitary-plus-projective-measurement paradigm.

Golden branch and canonical coding. The golden ratio $\varphi = (1 + \sqrt{5})/2$ and its inverse $\alpha = \varphi^{-1}$ play a privileged role. The golden rotation is maximally anti-resonant among irrational rotations (hardest to approximate by rationals), and it minimizes symbolic complexity within the binary Sturmian family. In this branch, Ostrowski numeration degenerates to the Zeckendorf decomposition: every $N \in \mathbb{N}$ admits a unique Fibonacci-sum representation with no adjacent terms [5–7].

2.2 Structural quantum gap: addition as lossy readout

A key HPA theorem is a no-go statement: beyond trivial cases, one cannot preserve both multiplicative structure and classical linear addition. We record the consequence in the form needed here.

Theorem 2.3 (No-go for simultaneous multiplicativity and linear additivity)**.** *Let $\Phi : \mathbb{N}_{>0} \to \mathbb{C}$ satisfy $\Phi(mn) = \Phi(m)\Phi(n)$ and $\Phi(a + b) = \Phi(a) + \Phi(b)$ for all $a, b, m, n \in \mathbb{N}_{>0}$. Then Φ is trivial (zero) or the identity embedding (up to the standard identification).*

Proof. Let $c := \Phi(1)$. By additivity, $\Phi(n) = \Phi(1 + \cdots + 1) = nc$ for all $n \in \mathbb{N}_{>0}$. By multiplicativity, $c = \Phi(1) = \Phi(1 \cdot 1) = \Phi(1)^2 = c^2$, hence $c \in \{0, 1\}$. If $c = 0$ then $\Phi \equiv 0$. If $c = 1$ then $\Phi(n) = n$ for all n, i.e. the standard embedding of $\mathbb{N}_{>0}$ into $\mathbb{C}$. □

Consequently, for a nontrivial multiplicative embedding $\mathcal{Z}$, the continuous vector synthesis $\mathcal{Z}(a) + \mathcal{Z}(b)$ is not constrained to lie on the discrete image $\mathcal{Z}(M)$. HPA models the induced additive operation as a readout projection (nearest-point, kernel projection, or a probabilistic instrument), and defines the *quantum gap* as the residual mismatch between synthesis and discrete coordinate recovery.

Definition 2.4 (Quantum gap (distance to the discrete image))**.** *Fix a multiplicative embedding $\mathcal{Z} : M \to \mathbb{C}$ and write $\mathcal{Z}(M) \subset \mathbb{C}$ for its discrete image. For a pair $(a, b) \in \mathbb{N}_{>0}^2$, define the quantum gap as the distance from continuous synthesis to the discrete image:*

$$\delta(a, b) \;:=\; \operatorname{dist}\big(\mathcal{Z}(a) + \mathcal{Z}(b),\, \mathcal{Z}(M)\big) \;:=\; \inf_{n \in \mathbb{N}_{>0}} \big\|\mathcal{Z}(a) + \mathcal{Z}(b) - \mathcal{Z}(n)\big\|. \tag{9}$$

Remark 2.5 (Readout rules as (approximate) minimizers)**.** *Any concrete readout protocol supplies a (possibly randomized) choice of an integer-valued map $\mathsf{R} : \mathbb{C} \to \mathbb{N}_{>0}$. If the infimum in Definition 2.4 is attained (or approximated), a natural deterministic readout is a nearest-image rule $\mathsf{R}_*(v) \in \arg\min_n \|v - \mathcal{Z}(n)\|$. More generally, any admissible readout R induces a residual $\delta_{\mathsf{R}}(a, b) := \|\mathcal{Z}(a) + \mathcal{Z}(b) - \mathcal{Z}(\mathsf{R}(\mathcal{Z}(a) + \mathcal{Z}(b)))\|$ with $\delta_{\mathsf{R}}(a, b) \geq \delta(a, b)$.*

The central point for this paper is conceptual: *space* enters not as a container but as the grammar and resolution of the readout protocol that discretizes a continuous ontological synthesis.

2.3 Omega Theory: PQCA microdynamics, exact 1D compilation, and lapse as routing overhead

We model microscopic evolution as a partitioned quantum cellular automaton (PQCA) on a quasi-local substrate with strictly local, finite-depth unitary updates. The PQCA viewpoint is compatible with standard QCA structure theorems (block representations and localizability) [8,9]. For the present paper we only use one interface theorem: any local PQCA step on a finite region can be compiled *exactly* into a one-dimensional nearest-neighbor circuit, and the minimal circuit depth becomes a computational notion of time.

Proposition 2.6 (Exact 1D nearest-neighbor compilation (Omega interface))**.** *Let U_R be a single local PQCA step restricted to a finite region R. There exist an encoding isometry E_R and a 1D nearest-neighbor circuit C_R such that*

$$U_R = E_R^\dagger C_R E_R. \tag{10}$$

Moreover, defining the routing overhead

$$\kappa(R) := \min_f \; \operatorname{depth}_{1\mathrm{D}}(U_R; f) \tag{11}$$

over 1D layouts/encodings f (Definition F.1), one may take $\operatorname{depth}(C_R) = \kappa(R)$. This overhead admits explicit, geometry-controlled bounds (Appendix F): for $n := |R|$ sites and bounded-degree local steps, $\kappa(R) = O(n)$ (Proposition F.5), while $\kappa(R) = \Omega(\operatorname{bw}(G_R))$ in terms of the interaction-graph bandwidth (Proposition F.2). In particular, for a d-dimensional L^d grid region, $\kappa(R) = \Omega(L^{d-1}) = \Omega(|\partial R|)$ (Theorem F.6).

At the circuit level, such compilations reduce to nearest-neighbor routing by swap networks; see Appendix F and, e.g., [10].

This motivates the *computational lapse* definition:

$$\mathcal{N}(x) := \frac{\kappa_0}{\kappa(x)}, \qquad d\tau_{\mathrm{loc}}(x) = \mathcal{N}(x)\, dt, \tag{12}$$

where t is measured in 1D nearest-neighbor depth and τ_{loc} counts locally realizable logical steps. In this language, "time dilation" is literally a slowdown in the implementable logical rate due to increased compilation/routing cost. Quantitative overhead bounds for standard geometries are summarized in Appendix F.

2.4 Undecidability interface: local reachability in universal QCA

The final interface fact is computability-theoretic. Universal QCAs can encode reversible computation; in Omega Theory this is sharpened into a local reachability predicate.

Theorem 2.7 (Undecidable local reachability in a universal QCA (Omega theorem))**.** *There exist a universal QCA update U and a family of initial states encoding instances (M, x) (a reversible machine M on input x), together with a finite region K and a local projector Π_K, such that the predicate*

$$\exists t \geq 0 : \ \langle \psi_{M,x} | \, U^{\dagger t} \, \Pi_K \, U^t \, | \psi_{M,x} \rangle > 0 \tag{13}$$

(i.e. whether the local flag Π_K is ever triggered) is algorithmically undecidable as a function of (M, x).

This theorem provides a strict mathematical pivot for later sections: "open-ended history" can be made precise as an undecidable reachability boundary within a strictly local, unitary microdynamics.

3 Complexity as physical cost: a unified resource semantics

This section performs two tasks: (i) it aligns standard complexity models with HPA–Ω objects, and (ii) it makes precise in what sense "time complexity *is* time" and "space complexity *is* space" in this framework: both are internal resource functionals of the scan–readout protocol.

3.1 Three standard models and their HPA–Omega alignment

Turing machine (TM). Time is step count $T(x)$; space is the number of tape cells visited $S(x)$.

Circuit model. Time is circuit depth $\mathrm{depth}(C)$; space is width / number of working wires.

Quantum cellular automaton (QCA). Time is the number of global update ticks t; space is active region size $|R|$ and local dimension d.

HPA–Omega alignment. The HPA scan iteration count k aligns with TM time and circuit depth:

$$T \sim k. \tag{14}$$

Readout prefix length N, canonical code length m (Ostrowski/Zeckendorf), and QCA active region $|R|$ align with space:

$$S \sim (N,\, m,\, |R|). \tag{15}$$

Omega Theory provides a further unification: local PQCA steps can be compiled to 1D nearest-neighbor circuits, so "time" can be expressed uniformly as nearest-neighbor depth.

3.2 Time complexity as an internal definition: scan depth and compilation depth

Definition 3.1 (Scan time complexity)**.** *Fix a scan operator Θ, an initial state $|\psi\rangle$, and a readout predicate P (for example, a predicate on the stabilized canonical code derived from the readout stream). For a tolerance $\epsilon > 0$, define the scan time complexity*

$$T_\Theta(P; \epsilon) := \min\Big\{ k \geq 0 : \ \mathrm{Readout}(\Theta^k |\psi\rangle) \ \textit{decides } P \ \textit{stably within error } \epsilon \Big\}. \tag{16}$$

If no such k exists, set $T_\Theta(P; \epsilon) = +\infty$.

Definition 3.2 (Compilation time complexity)**.** *For a finite region R and a local PQCA update U_R, define*

$$T_{\mathrm{comp}}(R) := \min_{f_R} \ \mathrm{depth}\big(C_R(f_R)\big), \tag{17}$$

where f_R ranges over admissible 1D layouts/encodings of R onto the tape and $C_R(f_R)$ is the corresponding 1D nearest-neighbor circuit implementing U_R (Proposition 2.6).

The lapse definition (12) is exactly the statement that local proper time is measured by the achievable logical rate per unit depth.

3.3 Space complexity as an internal definition: readout resolution and orthogonal cut capacity

Definition 3.3 (Readout space complexity)**.** *Fix a readout task* R *(e.g. reconstructing a canonical integer coordinate from the scan stream) and a tolerance $\epsilon > 0$. Let $s_0, \ldots, s_{N-1}$ be the binary stream induced by the window projection. Define*

$$S_{\mathrm{read}}(\mathsf{R}; \epsilon) := \min\Big\{ N \geq 1 : \ \textit{the length-}N\textit{ prefix suffices to complete } \mathsf{R} \textit{ within error } \epsilon \Big\}. \tag{18}$$

Definition 3.4 (Coding space complexity)**.** *Let* $\mathrm{Code}_\alpha(N)$ *denote the Ostrowski representation of N associated with slope α, and let $\ell(\mathrm{Code}_\alpha(N))$ be its digit length. Define*

$$S_{\mathrm{code}}(N; \alpha) := \ell\big(\mathrm{Code}_\alpha(N)\big). \tag{19}$$

In the golden branch $\alpha = \varphi^{-1}$, this specializes to the Zeckendorf digit length.

Definition 3.5 (QCA workspace complexity)**.** *For a QCA with local Hilbert dimension d and an active region R, define the workspace capacity*

$$S_{\mathrm{QCA}}(R) := |R| \log d. \tag{20}$$

In the scan–readout ontology, "space" is the minimal orthogonal grammar required to distinguish and stabilize readout outcomes. This is why the natural space measures are prefix length, canonical code length, and active-region capacity. Appendix E records explicit discrepancy and digit-depth scalings in the Sturmian/golden setting.

Proposition 3.6 (A concrete (T, S) scaling in the Sturmian scan model)**.** *In the window-scan model producing a mechanical word $s_0, \ldots, s_{N-1}$, the prefix-sum estimator $\widehat{\alpha}_N := S_N/N$ satisfies*

$$|\widehat{\alpha}_N - \alpha| < \frac{1}{N} \tag{21}$$

uniformly in N (Proposition E.1). Hence to achieve estimation error $\leq \epsilon$ it suffices to take $N \geq \lceil 1/\epsilon \rceil$ (Corollary E.2). Since one scan iteration produces one readout bit, the scan time to acquire an N-bit prefix scales as $T = \Theta(N)$ for such streaming tasks. In the golden branch, the corresponding Zeckendorf digit depth obeys $S_{\mathrm{code}} = \Theta(\log N) = \Theta(\log(\epsilon^{-1}))$ (Proposition E.4).

Remark 3.7 (A worked resource pipeline (example))**.** *For an estimation tolerance $\epsilon = 10^{-3}$, Corollary E.2 yields $N \geq 10^3$, so a streaming scan requires $T = \Theta(10^3)$ iterations to acquire the corresponding prefix. In the golden branch, Proposition E.4 gives a Zeckendorf digit depth on the order of*

$$m \ \gtrsim \ \log_\varphi\Big(\sqrt{5}\,\epsilon^{-1}\Big) \ \approx \ 16, \tag{22}$$

illustrating the separation between raw prefix length (streaming memory) and compressed canonical description length. Independently, for a 2D $L \times L$ grid region update, Theorem F.6 implies a compilation lower bound $\kappa(R) = \Omega(L)$ under 1D embedding; this is the quantitative sense in which geometry reappears as implementation-time overhead.

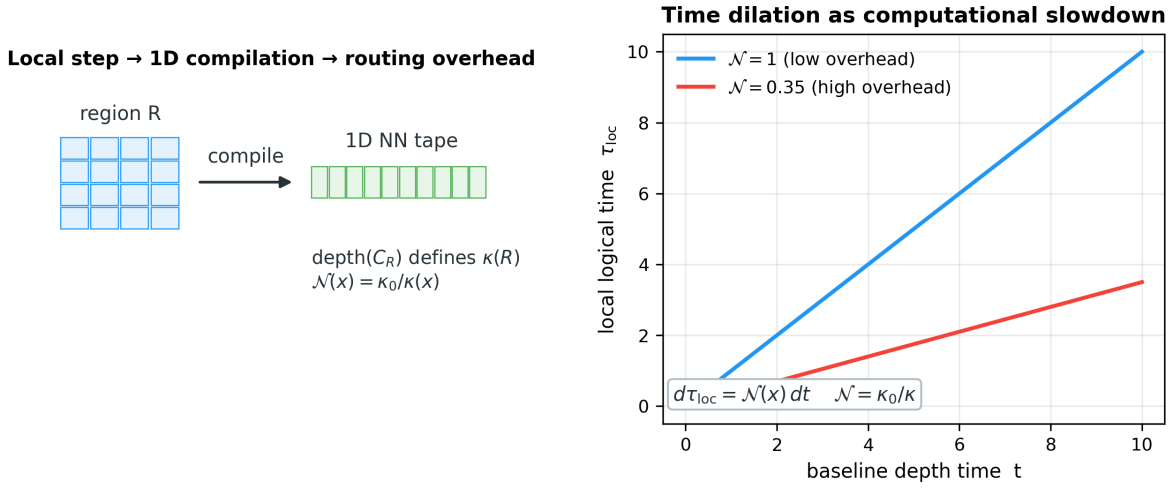

Figure 2: **Time complexity as scan/compilation depth and routing overhead.** A local PQCA step on a finite region can be implemented on a 1D nearest-neighbor tape at a depth cost that defines the routing overhead κ. The computational lapse $\mathcal{N} = \kappa_0/\kappa$ converts baseline depth time t into local logical time τ_{loc} via $d\tau_{\text{loc}} = \mathcal{N}(x)\,dt$.

4 Time complexity as geometric impedance: from scan iteration to emergent lapse

4.1 HPA: time as access order

In HPA, "time" is not a background parameter but the access order induced by the scan operator Θ: the system is accessed by the orbit $\{\Theta^k|\psi\rangle\}_{k\geq 0}$, and the physical content of "waiting longer" is the need for a larger iteration count before the readout stabilizes (Definition 3.1).

This internalization of time has a direct complexity interpretation: if a readout task requires deeper orbit sampling to resolve an ambiguity created by projection (or by phase aliasing), then the time cost is literally larger k.

4.2 Omega Theory: compilation overhead and time dilation as computational slowdown

Omega Theory adds a second, implementation-level notion of time: the depth required to implement a local update on a one-dimensional nearest-neighbor substrate (Definition 3.2). The key point is that an abstract "one-step" local PQCA update is not automatically a constant-time operation once one fixes a physical connectivity constraint (nearest neighbor). Routing induces overhead.

The lapse definition

$$\mathcal{N}(x) = \frac{\kappa_0}{\kappa(x)}, \qquad d\tau_{\text{loc}}(x) = \mathcal{N}(x)\,dt \tag{23}$$

states that the local proper time τ_{loc} counts realizable logical steps, while t counts baseline nearest-neighbor depth. Regions with larger routing overhead (κ large) execute fewer logical steps per unit t and therefore appear time-dilated.

4.3 Unitarity and reversible computation: why tradeoffs are structural

The scan and the QCA update are unitary and hence reversible. However, any nontrivial readout must involve projection, coarse graining, or conditioning—all of which are information-losing operations on the observed algebra. This juxtaposition reproduces, in a geometric language, a

standard phenomenon in reversible computation: simulating an irreversible computation reversibly typically forces a time–space tradeoff.

Bennett's pebbling-based results formalize this in the classical reversible setting [11]. In the present framework the tradeoff becomes transparent:

- Reducing *space* corresponds to using a shorter prefix, fewer orthogonal channels, or more aggressive projection.
- Reducing *time* corresponds to using fewer scan iterations or a shallower compiled circuit.

But the Weyl complementarity (Section 6) and the projection gap (Definition 2.4) imply that these reductions are incompatible beyond a structural limit: pushing readout resolution downward increases aliasing and instability, which then forces either more scan depth (time) or more workspace (space) to regain robustness.

In short, within HPA–Ω the phrase "time dilation" has an exact computational meaning: it is the slowdown induced by routing/compilation overhead required by locality constraints, coupled to readout-induced irreversibility.

5 Space complexity as readout resolution: from window cuts to canonical numeration

5.1 Readout produces a mechanical word: space as the cost of distinction

A window projection Π_W turns a continuous orbit into a binary stream $\{s_k\}$ (Equation (6)). This is the minimal observational alphabet: two outcomes corresponding to whether the phase lies inside the window. For irrational rotations with interval windows, the resulting sequence is Sturmian and has minimal factor complexity among aperiodic binary sequences:

$$p(n) = n + 1. \tag{24}$$

In other words, a Sturmian readout is a "least complex" way to encode a nonperiodic structure in a binary grammar [1, 2].

In the present language, *space* is the amount of grammar required to make distinctions stable. A longer prefix yields finer resolution because it refines the orbit partition and reduces discrepancy fluctuations (Equation (7)). Thus readout space complexity is naturally measured by prefix length (Definition 3.3); see Appendix E for explicit $O(1/N)$ discrepancy bounds.

5.2 Ostrowski and Zeckendorf: canonical coding as spatial resolution

The binary stream is not only a data record; in HPA it is also a coordinate system. Ostrowski numeration provides a canonical way to represent integers based on the continued fraction expansion of the slope α. In the golden branch $\alpha = \varphi^{-1}$ (continued fraction coefficients all equal to 1), Ostrowski representation degenerates to Zeckendorf representation: every $N \in \mathbb{N}$ has a unique Fibonacci-sum decomposition with no adjacent Fibonacci terms [5].

This is precisely why coding length is an appropriate space measure (Definition 3.4): a readout prefix of length N corresponds to a canonical digit string whose length is a discrete notion of spatial resolution.

5.3 Golden anti-resonance and coding minimality

Two extremal properties of the golden slope justify its role as a canonical "least locking" scan clock.

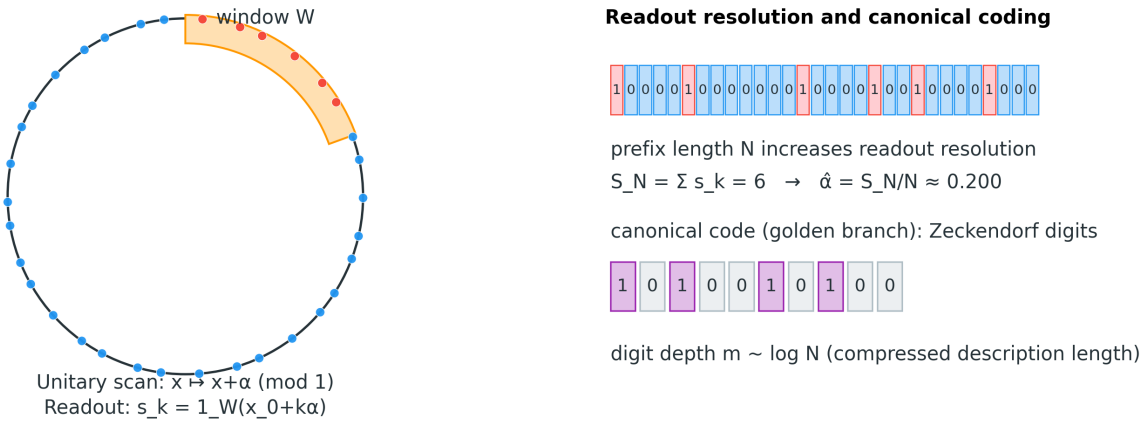

Figure 3: **Readout space complexity in the scan model.** A unitary scan on S^1 combined with a window projection Π_W produces a binary mechanical word s_k. Increasing the prefix length N improves readout resolution (Appendix E). In the golden branch, canonical Ostrowski coding degenerates to Zeckendorf coding, so the compressed digit depth scales as $m = \Theta(\log N)$.

- **Anti-resonance (Diophantine hardness).** The golden ratio is extremal for rational approximation: it is "worst approximable" in the Hurwitz sense (Appendix E), which minimizes phase lock-in and short periodic traps [6, 7].
- **Binary canonicality.** Continued fraction coefficients all equal to 1 yield the simplest Ostrowski constraints and hence the simplest canonical coding (Fibonacci/Zeckendorf).

Operationally: for fixed observational alphabet and fixed window grammar, the golden branch distributes orbit visits in a way that is simultaneously aperiodic and as non-resonant as possible, supporting stable readout without artificial periodicity.

5.4 Space is not a container but an orthogonal-cut syntax

The no-go theorem (Theorem 2.3) forces addition to be a readout, not an ontological operation. Hence every observable "coordinate" carries a memory of the cut that produced it. From this perspective, space complexity is the price of orthogonalization: increasing distinguishability requires either more channels (larger effective Hilbert workspace) or longer stabilization prefixes. This directly aligns with $S_{\mathrm{QCA}}(R) = |R| \log d$ (Definition 3.5) and with the view that dimension is a measurement grammar rather than a primitive container.

6 Time–space complementarity: Weyl-pair uncertainty as a resource lower bound

6.1 Weyl pairs in the scan model

Let $S^1 = \mathbb{R}/\mathbb{Z}$ and $\mathcal{H} = L^2(S^1, dx)$. Fix an irrational slope $\alpha \in \mathbb{R} \setminus \mathbb{Q}$. Define the scan shift

$$(Uf)(x) := f(x + \alpha), \tag{25}$$

and the phase multiplication operator

$$(Vf)(x) := \mathrm{e}^{2\pi \mathrm{i} x} f(x). \tag{26}$$

Then, by direct computation,

$$(UVf)(x) = \mathrm{e}^{2\pi \mathrm{i}(x+\alpha)} f(x + \alpha) = \mathrm{e}^{2\pi \mathrm{i}\alpha} (VUf)(x), \tag{27}$$

so U and V satisfy the Weyl relation

$$UV = \mathrm{e}^{\mathrm{i}\Phi} VU, \qquad \Phi := 2\pi\alpha. \tag{28}$$

Equivalently, U and V generate the irrational rotation algebra (the noncommutative torus) [12].

6.2 A variance-type uncertainty relation

Following Massar–Spindel [13] (see also the number–phase literature surveyed in [14] and the Pegg–Barnett approach [15]), define for a normalized state $|\psi\rangle$

$$\Delta_U^2 := 1 - \left|\langle\psi|U|\psi\rangle\right|^2, \qquad \Delta_V^2 := 1 - \left|\langle\psi|V|\psi\rangle\right|^2. \tag{29}$$

Then $\Delta_U = 0$ iff $|\psi\rangle$ is an eigenstate of U, and similarly for V. The Weyl commutation implies a quantitative obstruction to simultaneous eigenstate-like localization.

Theorem 6.1 (Weyl-pair complementarity (variance form))**.** *Let U, V be unitary operators satisfying $UV = \mathrm{e}^{\mathrm{i}\Phi} VU$, with the phase chosen so that $0 \le \Phi \le \pi$, and set $A = \tan(\Phi/2)$. Then for any normalized state $|\psi\rangle$,*

$$(1 + 2A)\,\Delta_U^2\,\Delta_V^2 + A^2\,(\Delta_U^2 + \Delta_V^2) \ge A^2. \tag{30}$$

In particular, if $\Phi \not\equiv 0 \bmod 2\pi$ then Δ_U and Δ_V cannot both be arbitrarily small.

Remark 6.2 (Closed-form vs tight unitary uncertainty bounds)**.** *Massar–Spindel [13] also provide a stronger (tight) characterization of the accessible region in the $(|\langle U\rangle|, |\langle V\rangle|)$ plane via the smallest eigenvalue of a Hermitian "Harper" operator (their Theorem 2). The present paper uses the closed-form inequality* (30) *because it yields an explicit algebraic tradeoff suitable for resource lower bounds and operational translation (Appendix B). Whenever tighter constants matter, one may replace* (30) *by the implicit Harper-eigenvalue boundary without changing the scan–readout semantics.*

6.3 Resource semantics: why T and S cannot both be minimized

Equation (30) becomes a resource statement once we identify U with scan access and V with readout phase channel.

- **Scan invariance and temporal resolution.** Small Δ_U means $|\psi\rangle$ is close to an eigenstate of the scan shift, so successive scan states have large overlap. Operationally, Δ_U is the trace distance between ρ and $U\rho U^\dagger$ for pure ρ (Appendix B), hence small Δ_U means it is difficult to distinguish "one tick" from "one tick plus a scan shift." In readout tasks that rely on accumulating distinguishable orbit information, such near-invariance typically forces larger scan depth.
- **Readout localization and phase-channel sharpness.** Small Δ_V means $|\psi\rangle$ is close to an eigenstate of the phase channel. Equivalently, the unitary conjugation $\rho \mapsto V\rho V^\dagger$ is hard to distinguish from ρ (Appendix B). In the scan–readout semantics this corresponds to sharpening distinctions in the readout/phase channel, which is generally paid for by increased readout resolution (longer prefixes and/or more orthogonal cut capacity).

Appendix B turns this into a concrete hypothesis-testing statement: the Helstrom-optimal binary decision errors for discriminating ρ from $U\rho U^\dagger$ and ρ from $V\rho V^\dagger$ obey the Weyl tradeoff (Proposition B.5).

A minimal $T(\epsilon)$ lower bound (task-level). As a canonical example, consider the decision problem of distinguishing whether a single scan shift has occurred, i.e. discriminating ρ from $U\rho U^\dagger$ for $U = \Theta$. For pure states, Appendix B gives an explicit n-copy Helstrom formula and an inversion: to achieve error $\leq \epsilon$ one needs at least

$$n \;\geq\; \frac{\log(1/(4\epsilon(1-\epsilon)))}{-\log(1-\Delta_U^2)} \;\gtrsim\; \frac{\log(1/\epsilon)}{\Delta_U^2}, \tag{31}$$

where $\Delta_U^2 = 1 - |\langle\psi|U|\psi\rangle|^2$ (Corollary B.8). Interpreting each repetition as one unit of scan access, this gives a concrete sense in which "near invariance under the scan" forces increased time cost for reliable discrimination.

Remark 6.3 (Resource accounting convention)**.** *The bound above is stated for n independent repetitions (or n identical copies) of the discrimination task. In this paper we use it as a minimal operational proxy for time cost: one repetition corresponds to one unit of experimental access to the scan–readout interface. This convention is standard in complexity-style resource accounting and is logically independent of any claims about obtaining multiple copies of a global universe state.*

The theorem says these objectives conflict when the scan is genuinely irrational (nontrivial Φ). Thus, in HPA–Ω, time–space tradeoffs are not engineering artifacts but formal consequences of (i) unitary access order and (ii) orthogonal projection readout.

This complements the reversible-computation tradeoff viewpoint (Section 4): unitarity preserves information globally, while readout discards information locally. The Weyl-pair constraint quantifies the irreducible incompatibility between "making access cheap" and "making distinctions sharp".

7 A quantum-cellular universe: 1D sufficiency, undecidability, and the observer as an interactive interface

7.1 Why the universe can be modeled as a QCA

A quantum cellular automaton (QCA) is a discrete-time, causal, unitary dynamics on a lattice (or graph) of finite-dimensional systems. Structure theorems show that unitarity plus causality implies implementability by local circuits ("localizability") [9], and reversible QCAs admit block representations in the sense of generalized Margolus partitionings [8]. It is a natural microdynamical carrier for three reasons: (i) it enforces finite propagation and locality (light-cone bounds for local quantum dynamics are formalized by Lieb–Robinson-type estimates [16]), (ii) it is exactly unitary (hence reversible), and (iii) it is computationally expressive: one-dimensional QCAs already support rich computation models [17], and intrinsically universal QCAs exist in higher dimensions [18]. In this manuscript we take QCA/PQCA as the microphysical substrate compatible with strict unitarity and locality constraints.

A complementary line of work studies continuum limits and emergent field dynamics in QCA/quantum-walk settings. Already early lattice-QCA constructions reproduce relativistic wave equations (Weyl/Dirac/Maxwell) as exact unitary updates with controlled lattice corrections [19]. More recent analyses make convergence to the Dirac equation explicit (including higher dimensions and observational convergence estimates) in discrete-time quantum walks [20, 21]. These results directly connect the QCA substrate to standard continuum kinematics and help situate scan-induced dispersion within the broader lattice-dispersion literature. At the same time, lattice fermion models face well-known obstructions such as fermion doubling in chiral settings [22], which constrains how continuum fields can emerge from strictly local, translation-invariant discretizations and motivates careful symmetry/encoding choices in any concrete QCA realization.

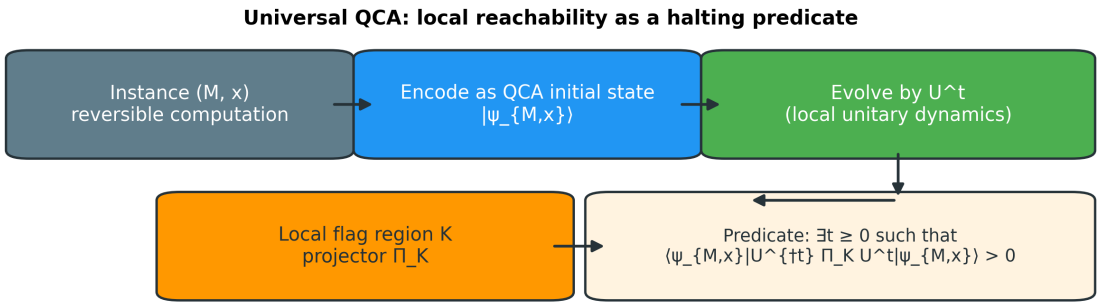

Figure 4: **Undecidable local reachability in a universal QCA.** A universal (reversible) computation instance (M, x) is encoded into an initial QCA state $|\psi_{M,x}\rangle$. A finite flag region K with projector Π_K records a halting-like event. The predicate $\exists t : \langle\psi_{M,x}|U^{\dagger t}\Pi_K U^t|\psi_{M,x}\rangle > 0$ reduces halting to local reachability (Appendix G).

7.2 Why one dimension is enough: geometry as compilation overhead

A recurring intuition is that "one-dimensional tape models are too thin to represent spacetime." The Omega interface theorem (Proposition 2.6) changes the meaning of "dimension" at the implementation layer: for any *finite* region update, there exists an exact 1D nearest-neighbor realization, and the cost of embedding higher adjacency into 1D is measured by routing overhead κ.

Thus, geometry need not be identified with the base dimension of the tape. Instead, geometry can be encoded as a *complexity field*: the overhead required to realize a given local logical step under a fixed connectivity constraint. This is precisely what the computational lapse $\mathcal{N}(x) = \kappa_0/\kappa(x)$ captures.

7.3 Undecidability as a theorem-level boundary

The undecidable reachability theorem (Theorem 2.7) has a direct conceptual reading. If a QCA is universal, then the question "will a certain localized event ever occur?" can be as hard as the halting problem. Hence, even in a completely unitary and local universe, there exist physically well-defined internal predicates whose long-time truth value is not decidable by any general algorithm.

This phenomenon is already present in classical cellular automata: many global properties and decision problems become undecidable once the dynamics can encode universal computation, and undecidability persists in reversible settings (see, e.g., [23, 24] for representative results). Theorem 2.7 is the unitary/QCA analogue tailored to the present interface: it packages undecidability as a local hitting predicate for a fixed causal update.

The reduction is given in Appendix G. In that precise sense, "open-ended history generation" can be stated without metaphor: there is no general algorithmic shortcut that decides all future local reachability events from the finite description of the initial encoding.

7.4 Observer = interactive machine + oracle-like interface (interpretation layer)

Up to this point, all claims are definition- or theorem-level. We now introduce an *interpretation edge*: a language for speaking about observation and selection without confusing it with a nonunitary modification of microdynamics.

Oracle language. Turing's ordinal-logic paper introduced oracle (o-machine) computation as a formalization of relative computability: an external predicate is treated as a resource that can be queried but not computed mechanically [25].

Interactive language. An observer in a QCA universe is not a one-shot function but a process that continually exchanges information with its environment. This motivates modeling observation as interactive computation, where the system's capability depends on continual input/output rather than on a single batch computation. (For broader discussions of interaction vs algorithms see e.g. [26].)

Selection as conditionalization. In the scan–readout ontology, "measurement" is a choice of cut and a conditioning on outcomes (a change of effective state on the observed algebra). When the conditioned predicate is undecidable as a function of the initial encoding, describing the selection step as an "oracle-like input" is a consistent interface language: it records that an additional resource (choice/conditioning) is being supplied from outside the purely algorithmic predictor.

Remark 7.1 (Strict layer separation)**.** *The undecidability theorem does* not *imply physical nonunitarity. It is a statement about the algorithmic decidability of certain internal reachability predicates. Modeling an observer as an interactive machine with oracle-like resources is a semantic choice: a way to talk about conditioning and resource injection at the readout level.*

This perspective allows one to phrase "collapse" as a statement about the readout history (conditionalization on a chosen branch) rather than as a modification of the global unitary dynamics.

8 Discrete-scan dispersion and the "speed of light" question

This section isolates one concrete, model-level interface between the scan formalism and phenomenology: the exact dispersion relation induced by a discrete scan/difference replacement. The goal is not to claim a unique physical prediction, but to provide a falsifiable template: any scan-based lattice model carries characteristic high-energy deviations from linear propagation. Related lattice-unitary models (QCA/quantum walks) derive relativistic wave equations with intrinsic lattice dispersion; see, e.g., [19, 20].

8.1 A representative exact dispersion relation

Replacing derivatives by finite differences at step size ε yields an exact lattice-type dispersion of the form

$$E(P) = \frac{2}{\varepsilon} \arcsin\left(\frac{\varepsilon P}{2}\right). \tag{32}$$

For $\varepsilon P \ll 1$, the low-energy expansion is

$$E(P) = P + \frac{\varepsilon^2 P^3}{24} + O(\varepsilon^4 P^5), \tag{33}$$

so linear propagation is recovered to leading order.

8.2 Derivation via the symbol of a symmetric difference

A compact derivation uses the standard Fourier symbol of the symmetric difference. Let the symmetric difference operator be

$$(\nabla_\varepsilon f)(t) := \frac{f(t+\varepsilon/2) - f(t-\varepsilon/2)}{\varepsilon}. \tag{34}$$

For a plane wave $f(t) = \exp(-\mathrm{i}Et)$ one has

$$\nabla_\varepsilon \exp(-\mathrm{i}Et) = -\mathrm{i}\,\widetilde{E}(E)\,\exp(-\mathrm{i}Et), \qquad \widetilde{E}(E) := \frac{2}{\varepsilon}\sin\!\left(\frac{\varepsilon E}{2}\right). \tag{35}$$

Imposing the continuum massless dispersion $E = P$ at the level of symbols by setting $\widetilde{E}(E) = P$ gives

$$\sin\!\left(\frac{\varepsilon E}{2}\right) = \frac{\varepsilon P}{2}, \tag{36}$$

which solves to Equation (32).

8.3 MDR form and the quadratic suppression scale

Squaring the low-energy expansion gives a convenient modified-dispersion-relation (MDR) form:

$$E^2 = P^2 + \frac{\varepsilon^2}{12}P^4 + O(\varepsilon^4 P^6). \tag{37}$$

Define the quadratic suppression scale

$$E_{\mathrm{QG},2} := \frac{\sqrt{12}}{\varepsilon}. \tag{38}$$

Then

$$E^2 = P^2\left[1 + \left(\frac{P}{E_{\mathrm{QG},2}}\right)^2 + O\!\left(\frac{P^4}{E_{\mathrm{QG},2}^4}\right)\right]. \tag{39}$$

This places the scan-induced dispersion directly into the standard quadratic LIV/MDR phenomenology vocabulary.

8.4 Group velocity and high-energy deviation

Differentiating (32) gives

$$\frac{dE}{dP} = \frac{1}{\sqrt{1-(\varepsilon P/2)^2}}. \tag{40}$$

Thus, the scan-induced dispersion predicts an energy-dependent deviation from constant group velocity. In particular, for $\varepsilon P \ll 1$,

$$\frac{dE}{dP} = 1 + \frac{\varepsilon^2 P^2}{8} + O(\varepsilon^4 P^4) \;=\; 1 + \frac{3}{2}\left(\frac{P}{E_{\mathrm{QG},2}}\right)^2 + \cdots. \tag{41}$$

8.5 Cosmological time-of-flight fitting (quadratic case)

For a source at redshift z in a standard FRW background, the leading quadratic time-delay template takes the familiar form [27]:

$$\Delta t_{\mathrm{LIV}} \;\simeq\; s_2\,\frac{3}{2}\,\frac{E_{\mathrm{h},0}^2 - E_{\mathrm{l},0}^2}{E_{\mathrm{QG},2}^2}\int_0^z \frac{(1+z')^2}{H(z')}\,dz', \tag{42}$$

where $E_{\mathrm{h},0}, E_{\mathrm{l},0}$ are the observed photon energies and $s_2 \in \{+1, -1\}$ encodes subluminal vs superluminal sign conventions. Here $H(z)$ is the Hubble parameter; for a spatially flat ΛCDM background one may take

$$H(z) = H_0\sqrt{\Omega_m(1+z)^3 + \Omega_\Lambda}. \tag{43}$$

In the scan dispersion (32), the quadratic correction is superluminal (positive $dE/dP - 1$), corresponding to a fixed sign choice in this template.

Equation (42) provides a direct fitting pipeline: given $(\Delta t_i, E_{\mathrm{h},0,i}, E_{\mathrm{l},0,i}, z_i)$ one can regress for $E_{\mathrm{QG},2}$ (equivalently ε via (38)) subject to astrophysical emission-lag systematics.

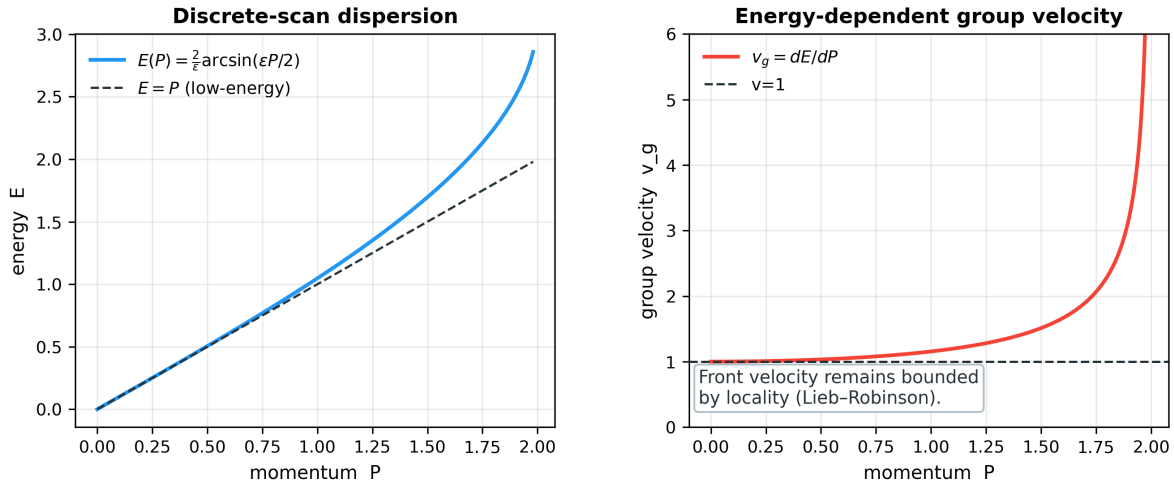

Figure 5: **Discrete-scan dispersion and energy-dependent group velocity.** The exact scan-induced dispersion $E(P) = \frac{2}{\varepsilon}\arcsin(\varepsilon P/2)$ is approximately linear at low energy and deviates at high momentum. The corresponding group velocity $v_g = dE/dP$ becomes energy-dependent; microscopic locality in a QCA/PQCA imposes a separate signal/front-velocity bound (Lieb–Robinson).

8.6 A concrete bound (example)

Using Fermi-LAT gamma-ray burst data, Vasileiou *et al.* reported a robust quadratic constraint of order

$$E_{\mathrm{QG},2} > 1.3 \times 10^{11}\,\mathrm{GeV} \tag{44}$$

within their systematic treatment [28] (see also the earlier GRB 090510 limit [29]). Translating via (38) gives the corresponding bound on the scan step

$$\varepsilon < \frac{\sqrt{12}}{1.3 \times 10^{11}\,\mathrm{GeV}} \approx 2.7 \times 10^{-11}\,\mathrm{GeV}^{-1}. \tag{45}$$

In length units, $1\,\mathrm{GeV}^{-1} \simeq 1.97 \times 10^{-16}\,\mathrm{m}$, so $\varepsilon \lesssim 5.3 \times 10^{-27}\,\mathrm{m}$.

8.7 Translating GRB 090510 timing limits into the quadratic scale

Equation (42) can be inverted to obtain a one-sided lower limit on $E_{\mathrm{QG},2}$ (hence an upper limit on ε) from any published time-delay constraint. For a single event with observed energies $E_{\mathrm{h},0}, E_{\mathrm{l},0}$ at redshift z and an upper bound $|\Delta t| \le \Delta t_{\max}$, one obtains

$$E_{\mathrm{QG},2} \;>\; \left[\frac{3}{2}\,\frac{E_{\mathrm{h},0}^2 - E_{\mathrm{l},0}^2}{\Delta t_{\max}}\left(\int_0^z \frac{(1+z')^2}{H(z')}\,dz'\right)\right]^{1/2}, \tag{46}$$

which is a conservative one-sided bound obtained from the absolute time-delay constraint (independent of the sign convention). Abdo *et al.* [29] tabulate a set of conservative and less-conservative upper bounds on $|\Delta t|$ for GRB 090510 based on different choices of the reference emission time (their Table 2). Using a standard flat ΛCDM background in the integral, these bounds translate to quadratic limits on $E_{\mathrm{QG},2}$ and ε that are consistent (in order of magnitude) with the later systematic analysis [28].

Constraint source	$\Delta t_{\max}$ (ms)	$E_{\mathrm{QG},2}$ lower bound (GeV)	ε upper bound (GeV^{-1})
GRB 090510, conservative onset choice (Table 2a) [29]	859	3.0×10^{10}	1.1×10^{-10}
GRB 090510, $> 1\,\mathrm{GeV}$ onset choice (Table 2d) [29]	99	8.9×10^{10}	3.9×10^{-11}
GRB 090510, spike association (Table 2e) [29]	10	2.8×10^{11}	1.2×10^{-11}
Fermi-LAT systematic quadratic bound [28]	—	1.3×10^{11}	2.7×10^{-11}

Table 2: **Representative published timing constraints translated into the quadratic scan scale.** The GRB 090510 entries are obtained by combining the published $\Delta t_{\max}$ values [29] with the quadratic time-of-flight template (42); the corresponding ε bound uses (38). The numerical translation uses $z = 0.900$ and the 1σ lower energy $E_{\mathrm{h},0} = 28\,\mathrm{GeV}$ reported in [29], with the low-energy reference chosen as in their Table 2, and a standard flat ΛCDM background in the redshift integral (e.g. $H_0 \simeq 67.4\,\mathrm{km\,s^{-1}\,Mpc^{-1}}$, $\Omega_m \simeq 0.315$). Results depend only weakly on the background cosmology.

8.8 A reproducible likelihood template for fitting ε (quadratic case)

Given a dataset of observed spectral lags Δt_i with uncertainties σ_i and associated $(E_{\mathrm{h},0,i}, E_{\mathrm{l},0,i}, z_i)$, define the regressor

$$X_i \;:=\; \left(E_{\mathrm{h},0,i}^2 - E_{\mathrm{l},0,i}^2\right) \int_0^{z_i} \frac{(1+z')^2}{H(z')}\, dz'. \tag{47}$$

Introduce the parameter $\eta := s_2\, E_{\mathrm{QG},2}^{-2}$ (equivalently $\varepsilon = \sqrt{12}\, E_{\mathrm{QG},2}^{-1}$). Then the leading quadratic model is

$$\Delta t_i \;=\; \Delta t_{\mathrm{int},i} \;+\; \frac{3}{2}\,\eta\, X_i \;+\; \epsilon_i, \tag{48}$$

where $\Delta t_{\mathrm{int},i}$ captures intrinsic source emission lags and ϵ_i is observational noise. A standard conservative treatment is to model $\Delta t_{\mathrm{int},i}$ as a nuisance term (either per-burst intercepts or a hierarchical distribution) and to include an intrinsic-scatter parameter σ_{int}. For Gaussian errors, one convenient log-likelihood is

$$\log L(\eta, \{\Delta t_{\mathrm{int}}\}, \sigma_{\mathrm{int}}) = -\frac{1}{2} \sum_i \left[\frac{\left(\Delta t_i - \Delta t_{\mathrm{int},i} - \frac{3}{2}\eta X_i\right)^2}{\sigma_i^2 + \sigma_{\mathrm{int}}^2} + \log(\sigma_i^2 + \sigma_{\mathrm{int}}^2) \right]. \tag{49}$$

This template makes explicit what is and is not being assumed: constraints on ε tighten only to the extent that intrinsic-lag systematics can be controlled (e.g. by within-burst association methods, by multi-pulse modeling, or by hierarchical pooling).

8.9 Causality: group velocity vs signal velocity

Equation (40) can exceed 1 for sufficiently large P. However, in a strictly local update model (QCA/PQCA), information propagation is bounded by locality: per tick, influence can spread only within a finite neighborhood. In fact, for a causal QCA with neighborhood radius r, the Heisenberg evolution obeys a *strict* light-cone statement [9]:

$$\mathrm{supp}\left(U^\dagger A_X U\right) \subseteq \mathcal{N}_r(X), \tag{50}$$

for any observable A_X supported on a finite set X, where $\mathcal{N}_r(X)$ denotes the r-neighborhood of X in graph distance. Iterating gives $\mathrm{supp}(U^{-t} A_X U^t) \subseteq \mathcal{N}_{rt}(X)$, so the front/signal velocity is bounded by the microscopic causality radius. For more general local quantum dynamics generated by Hamiltonians, strict causality is replaced by an exponentially suppressed tail outside

an effective cone, formalized by Lieb–Robinson bounds [16]. Therefore, an apparent "superluminal group velocity" extracted from a lattice dispersion must be interpreted cautiously: group velocity is not a signal-velocity guarantee, while the microscopic locality constraint enforces the true causal speed limit.

8.10 How this connects back to complexity

In the unified semantics, the effective propagation speed is determined by the scan step and by the compilation overhead required to realize local updates. Hence, "light-cone structure" is itself a complexity statement: it is a bound on how many sites can be causally reached within a given depth budget. This ties the phenomenological dispersion discussion back to the central theme: kinematics is constrained by scan complexity (iteration/depth) and by readout resolution (which determines which deviations are operationally accessible).

8.11 Laboratory constraints and operator content

It is important to distinguish which kind of Lorentz-violation tests apply to which operator structures. The scan-induced MDR in (37) is an *isotropic, energy-dependent* modification of propagation (quadratic in energy at leading order). At optical or microwave energies, the relative correction is suppressed by $(E/E_{\mathrm{QG},2})^2$. For example, taking $E \sim 1\,\mathrm{eV}$ and $E_{\mathrm{QG},2} \gtrsim 10^{11}\,\mathrm{GeV}$ yields $(E/E_{\mathrm{QG},2})^2 \lesssim 10^{-40}$, far below laboratory sensitivity. Accordingly, precision cavity experiments are most constraining for *anisotropic* and/or polarization-dependent modifications (SME-type operator coefficients) rather than for an isotropic $n = 2$ time-of-flight term; see the review [30] and representative optical-resonator tests such as [31]. This is why high-energy, long-baseline time-of-flight observations dominate the quantitative bounds quoted in Table 2 for the present MDR template.

9 Computational teleology and cybernetics: an open-ended universe near the undecidability boundary

9.1 Teleology as a computable objective: sustaining open-endedness

Once undecidable reachability predicates exist (Theorem 2.7), the phrase "the universe aims to compute an ultimate answer and halt" is not the natural fixed point. A more precise statement is available: for finite-resource observers, what matters is whether the scan–readout protocol continues to generate histories that are simultaneously (i) not trapped in short periodic loops (overly decidable/compressible) and (ii) not washed out into pure noise (unreadable/incompressible).

We package this as a definition at the interpretation/interface layer.

Definition 9.1 (Computational teleology (interface definition))**.** *A unitary scan–readout universe exhibits* computational teleology *if its effective operation stabilizes a regime in which*

- ***Expressivity:*** *local reachability remains rich enough to support undecidable predicates (open-endedness);*
- ***Legibility:*** *finite-resource observers can extract stable, compressible, and actionable readout histories.*

Equivalently, teleology is an operational balance between undecidability (expressivity) and readout feasibility (resource-bounded distinguishability).

9.2 Golden anti-resonance as a control law

The golden branch supplies a particularly rigid "control" mechanism: it avoids phase lock-in (anti-resonance) while minimizing symbolic complexity (binary Sturmian minimality), thus generating a clock texture that is neither periodic nor maximally random. In the present language, this is a resource-control statement: golden coding minimizes the space overhead needed to avoid resonant collapse of the scan dynamics.

9.3 Complexity classes: what can and cannot be claimed

It is tempting to map physical motifs directly onto complexity-class conjectures (e.g. to treat "persistent matter" as evidence of class separations such as $\mathrm{P} \neq \mathrm{NP}$). Such statements are not acceptable as theorem-level claims, because the conjectures are open.

What *is* acceptable is a carefully separated analogy: interaction can boost verification power in the standard interactive-proof setting [32], culminating in the theorem $\mathrm{IP} = \mathrm{PSPACE}$ [33]. In an observer-as-interactive-machine picture (Section 7.4), one may view the environment as a prover-like stream and the observer as a verifier-like process constrained by (T, S). This does not prove any new separation, but it clarifies how "verification" and "construction" may have different resource profiles in a scan–readout universe.

9.4 A cybernetic reading

In cybernetic terms, the observer is a controller operating under resource constraints. The scan supplies an access channel; the projection supplies a compression channel; undecidability supplies a hard boundary on prediction; and the control objective is to keep the system in a regime where prediction is neither trivial nor impossible. This yields a concrete, publication-friendly version of "teleology": not metaphysical purpose, but resource-stabilized open-ended operation.

10 Conclusion and outlook

We organized Holographic Polar Arithmetic and Omega Theory into a single operational chain connecting computation, geometry, and observation. The central move is definitional: time and space are internal resource costs of a scan–readout protocol.

Time. Time complexity becomes physical time in two equivalent guises: scan depth (iteration count of Θ) and 1D compilation depth (nearest-neighbor circuit depth implementing a local PQCA step). The Omega lapse $\mathcal{N}(x) = \kappa_0/\kappa(x)$ makes time dilation an explicit computational slowdown induced by routing overhead.

Space. Space complexity becomes readout resolution: the prefix length and canonical digit depth required to stabilize a coordinate under projection readout, together with the active-region workspace capacity $|R| \log d$.

Tradeoffs. A Weyl-pair uncertainty relation provides a hard complementarity between scan-localization and readout-localization, and reversible-computation theory explains why projection readout forces time–space tradeoffs rather than optional engineering compromises.

Open-endedness. Universal QCAs support undecidable local reachability predicates, supplying a theorem-level boundary for "open-ended history." Modeling observers as interactive machines with oracle-like resources is an interpretation-layer interface that keeps unitary microdynamics intact.

Testability. Discrete scan dynamics induces an exact lattice dispersion relation: it is approximately linear at low energy and deviates at high momentum, providing a falsifiable template for energy-dependent propagation.

Future directions

Two technically sharp directions follow from this organization.

- **Quantitative $(T(\epsilon), S(\epsilon))$ bounds.** Derive explicit upper/lower bounds for stabilization time and readout space at tolerance ϵ, connecting discrepancy control (Denjoy–Koksma/Ostrowski bounds) to complexity lower-bound techniques.
- **Linking κ to observables.** Establish a more direct quantitative bridge from routing overhead $\kappa(x)$ to effective gravitational observables (time-delay, redshift templates), with controlled approximations and explicit error budgets.

A Complexity–geometry dictionary

For convenience we collect the main identifications used throughout the paper.

1. **Scan time.** $k \in \mathbb{Z}_{\geq 0}$, iteration count of the unitary scan Θ^k.
2. **Readout operator.** Window projection Π_W producing binary readout bits $s_k \in \{0, 1\}$.
3. **Readout resolution.** Prefix length N and canonical code length m (Ostrowski digit depth; Zeckendorf in the golden branch).
4. **Compilation time.** 1D nearest-neighbor circuit depth $\mathrm{depth}(C_R)$ implementing a local PQCA step on region R.
5. **Routing overhead.** $\kappa(x)$, the overhead functional controlling depth under 1D embedding; computational lapse $\mathcal{N}(x) = \kappa_0/\kappa(x)$.
6. **Workspace capacity.** $S_{\mathrm{QCA}}(R) = |R| \log d$ for local dimension d.
7. **Undecidability pivot.** Local reachability predicate "$\exists t : \Pi_K$ triggers" is undecidable in a universal QCA.

B From Weyl pairs to resource complementarity: inequality and operational meaning

We record the minimal objects behind the variance-form uncertainty inequality used in Theorem 6.1. The inequality (in essentially this form) is due to Massar–Spindel [13] for unitary operators obeying a Weyl commutation relation; for completeness we include a self-contained derivation (following their proof of Theorem 1 in [13]).

Weyl relation. Let U, V be unitaries satisfying $UV = \mathrm{e}^{\mathrm{i}\Phi} VU$. Nontrivial Φ implies U and V cannot be simultaneously diagonalized.

Unitary variances. For a normalized state $|\psi\rangle$, define

$$\Delta_U^2 = 1 - |\langle U \rangle|^2, \qquad \Delta_V^2 = 1 - |\langle V \rangle|^2, \tag{51}$$

where $\langle U \rangle := \langle \psi | U | \psi \rangle$. These vanish exactly on eigenstates.

B.1 Proof of Theorem 6.1 (Massar–Spindel inequality)

We assume the phase is chosen so that $0 \le \Phi \le \pi$ (this can always be arranged without changing Δ_U, Δ_V by replacing U or V with its adjoint, which flips $\Phi \mapsto -\Phi$ modulo 2π). Set

$$A := \tan(\Phi/2) \;\ge\; 0. \tag{52}$$

Sine/cosine operators. Introduce the Hermitian operators

$$C_U := \frac{U+U^\dagger}{2}, \quad S_U := \frac{U-U^\dagger}{2\mathrm{i}}, \qquad C_V := \frac{V+V^\dagger}{2}, \quad S_V := \frac{V-V^\dagger}{2\mathrm{i}}. \tag{53}$$

They satisfy $C_U^2 + S_U^2 = \mathbb{1}$ and $C_V^2 + S_V^2 = \mathbb{1}$. Moreover,

$$\Delta_U^2 = \Delta C_U^2 + \Delta S_U^2, \qquad \Delta_V^2 = \Delta C_V^2 + \Delta S_V^2, \tag{54}$$

where $\Delta X^2 := \langle X^2\rangle - \langle X\rangle^2$ for Hermitian X.

Robertson reduction. Since $\Delta_U^2 \ge \Delta S_U^2$ and $\Delta_V^2 \ge \Delta S_V^2$, one has

$$\Delta_U^2 \Delta_V^2 \;\ge\; \Delta S_U^2 \, \Delta S_V^2. \tag{55}$$

By the Robertson uncertainty relation, for any Hermitian A, B,

$$\Delta A \, \Delta B \;\ge\; \frac{1}{2}|\langle [A,B]\rangle|, \tag{56}$$

and therefore

$$\Delta_U^2 \Delta_V^2 \;\ge\; \frac{1}{4}|\langle [S_U, S_V]\rangle|^2. \tag{57}$$

Lemma B.1 (Sine-commutator identity [13, Proof of Theorem 1])**.** *If U, V satisfy $UV = \mathrm{e}^{\mathrm{i}\Phi} VU$ with $0 \le \Phi \le \pi$ and $A = \tan(\Phi/2)$, then*

$$[S_U, S_V] = -\mathrm{i}A\,(C_U C_V + C_V C_U). \tag{58}$$

Proof. Using (53) one expands

$$S_U S_V = -\frac{1}{4}\,(UV + U^\dagger V^\dagger) + \frac{1}{4}\,(U^\dagger V + UV^\dagger), \tag{59}$$

$$S_V S_U = -\frac{1}{4}\,(VU + V^\dagger U^\dagger) + \frac{1}{4}\,(V^\dagger U + VU^\dagger), \tag{60}$$

$$C_U C_V = \frac{1}{4}\,(UV + U^\dagger V^\dagger) + \frac{1}{4}\,(U^\dagger V + UV^\dagger), \tag{61}$$

$$C_V C_U = \frac{1}{4}\,(VU + V^\dagger U^\dagger) + \frac{1}{4}\,(V^\dagger U + VU^\dagger). \tag{62}$$

Using $UV = \mathrm{e}^{\mathrm{i}\Phi} VU$ and $U^\dagger V = VU^\dagger \mathrm{e}^{-\mathrm{i}\Phi}$ to rewrite terms yields two equivalent forms:

$$[S_U, S_V] = -\mathrm{i}\sin\Phi\, C_V C_U - 2\sin^2(\Phi/2)\, S_V S_U, \tag{63}$$

$$[S_U, S_V] = -\mathrm{i}\sin\Phi\, C_U C_V + 2\sin^2(\Phi/2)\, S_U S_V. \tag{64}$$

Combining them gives

$$[S_U, S_V] = -\mathrm{i}\,\frac{\sin\Phi}{2\cos^2(\Phi/2)}\,(C_U C_V + C_V C_U) \;=\; -\mathrm{i}\tan(\Phi/2)\,(C_U C_V + C_V C_U), \tag{65}$$

as claimed. □

Lemma B.2 (Lower bound on $\langle C_U C_V\rangle$ [13, Proof of Theorem 1])**.** *By rephasing $U \mapsto \mathrm{e}^{-\mathrm{i}\arg\langle U\rangle}U$ and $V \mapsto \mathrm{e}^{-\mathrm{i}\arg\langle V\rangle}V$ one may assume $\langle U\rangle, \langle V\rangle \in \mathbb{R}_{\geq 0}$, hence $\langle S_U\rangle = \langle S_V\rangle = 0$ and $\langle C_U\rangle = \sqrt{1-\Delta_U^2}$, $\langle C_V\rangle = \sqrt{1-\Delta_V^2}$. With this choice,*

$$\big|\langle C_U C_V\rangle\big| \;\geq\; \sqrt{1-\Delta_U^2}\,\sqrt{1-\Delta_V^2} - \Delta_U\Delta_V. \tag{66}$$

Proof. Write $C_U|\psi\rangle = x_U|\psi\rangle + y_U|\psi^\perp\rangle$ where $|\psi^\perp\rangle$ is normalized and orthogonal to $|\psi\rangle$, and $x_U = \langle C_U\rangle$. Since $\|C_U\| \leq 1$, one has $x_U^2 + y_U^2 = \langle\psi|C_U^2|\psi\rangle \leq 1$, hence $y_U^2 \leq 1 - x_U^2 = \Delta_U^2$. Similarly, $C_V|\psi\rangle = x_V|\psi\rangle + y_V|\psi'^\perp\rangle$ with $x_V = \langle C_V\rangle$ and $y_V^2 \leq \Delta_V^2$. Therefore

$$\begin{aligned}
\big|\langle C_V C_U\rangle\big| &= |x_U x_V + y_U y_V \langle\psi'^\perp|\psi^\perp\rangle| && (67)\\
&\geq x_U x_V - |y_U y_V| && (68)\\
&\geq \sqrt{1-\Delta_U^2}\,\sqrt{1-\Delta_V^2} - \Delta_U\Delta_V, && (69)
\end{aligned}$$

which implies (66). □

Proof of Theorem 6.1. Using Lemma B.1 in (57) gives

$$\Delta_U\Delta_V \;\geq\; A\,\big|\langle C_U C_V\rangle\big|. \tag{70}$$

Applying Lemma B.2 yields

$$\Delta_U\Delta_V \;\geq\; A\Big(\sqrt{1-\Delta_U^2}\,\sqrt{1-\Delta_V^2} - \Delta_U\Delta_V\Big). \tag{71}$$

Rearranging and squaring (71) gives (30). □

Resource reading. In the scan model, $U = \Theta$ encodes access order (time), while V encodes phase/readout channels (space). The inequality asserts that sharpening readout localization (small Δ_V) forces scan delocalization (large Δ_U), and vice versa. This is the formal kernel of time–space resource complementarity.

B.2 Operational meaning: overlap, trace distance, and binary decision error

The variance quantities Δ_U, Δ_V admit a direct operational meaning in quantum hypothesis testing. Let $\rho := |\psi\rangle\langle\psi|$ be a pure state and define the unitary conjugates

$$\rho_U := U\rho U^\dagger, \qquad \rho_V := V\rho V^\dagger. \tag{72}$$

Write the trace distance as $D(\rho,\sigma) := \frac{1}{2}\|\rho-\sigma\|_1$, where $\|X\|_1 := \mathrm{Tr}\sqrt{X^\dagger X}$ [3].

Lemma B.3 (Unitary variance equals trace distance for pure states)**.** *For any normalized $|\psi\rangle$ and unitary U,*

$$D(\rho,\rho_U) = \sqrt{1-\big|\langle\psi|U|\psi\rangle\big|^2} = \Delta_U. \tag{73}$$

The analogous identity holds with U replaced by V.

Proof. For pure states $\rho = |\psi\rangle\langle\psi|$ and $\sigma = |\phi\rangle\langle\phi|$ one has the standard formula $D(\rho,\sigma) = \sqrt{1-|\langle\psi|\phi\rangle|^2}$ [3]. Taking $|\phi\rangle := U|\psi\rangle$ yields $D(\rho,\rho_U) = \sqrt{1-|\langle\psi|U|\psi\rangle|^2}$. □

Corollary B.4 (Helstrom error for distinguishing a unitary conjugate)**.** *Consider binary discrimination between ρ and ρ_U with equal prior probabilities. The optimal (minimum) error probability is given by the Helstrom formula [3, 34]*

$$p_{\mathrm{err}}^*(U;\psi) = \frac{1}{2}\left(1 - D(\rho,\rho_U)\right) = \frac{1}{2}\left(1-\Delta_U\right). \tag{74}$$

Equivalently, $\Delta_U = 1 - 2p_{\mathrm{err}}^*(U;\psi)$. The same statement holds for V with Δ_V.

Thus, Δ_U measures how distinguishable successive scan states are (one tick vs one tick plus a scan shift), while Δ_V measures how distinguishable the phase/readout channel is under conjugation by the phase operator.

B.3 A task-level tradeoff induced by the Weyl inequality

Combine Theorem 6.1 with Corollary B.4. Define the optimal equal-prior error probabilities

$$p_U := p^*_{\mathrm{err}}(U;\psi), \qquad p_V := p^*_{\mathrm{err}}(V;\psi). \tag{75}$$

Then $\Delta_U = 1 - 2p_U$ and $\Delta_V = 1 - 2p_V$.

Proposition B.5 (Binary-decision tradeoff for a Weyl pair)**.** *Let U, V satisfy $UV = \mathrm{e}^{\mathrm{i}\Phi}VU$, with the phase chosen so that $0 \le \Phi \le \pi$, and set $A = \tan(\Phi/2)$. For any normalized state $|\psi\rangle$, the optimal discrimination errors p_U, p_V satisfy*

$$(1+2A)\,(1-2p_U)^2(1-2p_V)^2 + A^2\big((1-2p_U)^2 + (1-2p_V)^2\big) \;\ge\; A^2. \tag{76}$$

Equivalently, in terms of Δ_U, Δ_V the inequality is exactly (30)*.*

Remark B.6 (How this functions as a resource lower bound)**.** *Equation* (76) *is a concrete, task-level statement: one cannot simultaneously make both unitary conjugations U and V "almost invisible" to the state (i.e. $p_U \approx p_V \approx \frac{1}{2}$). In the scan–readout semantics, making the readout channel sharp pushes the state toward a regime where the V-conjugation is hard to detect (small Δ_V), which forces scan shifts to be detectable (large Δ_U), and vice versa. This tradeoff underlies the impossibility of jointly optimizing access (scan) and distinction (readout) in a single state preparation.*

B.4 From distinguishability to a sample-complexity lower bound

The preceding identities are single-shot statements. To translate them into a time-like resource, one may consider repeating the same discrimination task with n identical copies (or, equivalently, n independent repetitions of state preparation and measurement).

Proposition B.7 (Helstrom error for n copies of pure states)**.** *Let $\rho_0 = |\psi_0\rangle\langle\psi_0|$ and $\rho_1 = |\psi_1\rangle\langle\psi_1|$ be pure states with equal priors. For n copies, the optimal (minimum) error probability for distinguishing $\rho_0^{\otimes n}$ from $\rho_1^{\otimes n}$ is*

$$p^{*(n)}_{\mathrm{err}}(\psi_0,\psi_1) = \frac{1}{2}\left(1 - \sqrt{1 - |\langle\psi_0|\psi_1\rangle|^{2n}}\right). \tag{77}$$

Proof. The Helstrom formula gives $p^{*(n)}_{\mathrm{err}} = \frac{1}{2}(1 - D(\rho_0^{\otimes n}, \rho_1^{\otimes n}))$ [3, 34]. For pure states one has $D(\rho,\sigma) = \sqrt{1 - F(\rho,\sigma)}$ with $F(\rho,\sigma) = |\langle\psi|\phi\rangle|^2$ [3]. Since $|\langle\psi_0^{\otimes n}|\psi_1^{\otimes n}\rangle|^2 = |\langle\psi_0|\psi_1\rangle|^{2n}$, the claim follows. □

Corollary B.8 (Copies needed to detect a unitary conjugation)**.** *Let $\rho = |\psi\rangle\langle\psi|$ and $\rho_U = U\rho U^\dagger$ with overlap $F_U := |\langle\psi|U|\psi\rangle|^2 = 1 - \Delta_U^2$. For any target error $\epsilon \in (0, \frac{1}{2})$, achieving $p^{*(n)}_{\mathrm{err}}(U;\psi) \le \epsilon$ requires*

$$n \;\ge\; \frac{\log(1/(4\epsilon(1-\epsilon)))}{-\log F_U} \;=\; \frac{\log(1/(4\epsilon(1-\epsilon)))}{-\log(1-\Delta_U^2)}. \tag{78}$$

If $\Delta_U = 0$ (equivalently $F_U = 1$), then $\rho = \rho_U$ and no finite n can reduce the optimal error below $1/2$. In particular, for $\Delta_U^2 \ll 1$ one has $-\log(1-\Delta_U^2) = \Delta_U^2 + O(\Delta_U^4)$, so

$$n \;\gtrsim\; \frac{\log(1/\epsilon)}{\Delta_U^2}. \tag{79}$$

Proof. By (77), the condition $p^{*(n)}_{\mathrm{err}} \le \epsilon$ is equivalent to $|\langle\psi|U|\psi\rangle|^{2n} \le 4\epsilon(1-\epsilon)$. Taking logarithms yields (78). The asymptotic expansion uses $-\log(1-x) = x + O(x^2)$. □

Corollary B.8 makes the "small Δ_U implies expensive time" intuition precise for a canonical task: if a scan shift is almost invisible to the state (small Δ_U), then the number of independent repetitions required to achieve error $\le \epsilon$ must grow at least on the order of $\log(1/\epsilon)/\Delta_U^2$.

C Ostrowski/Zeckendorf numeration and readout space complexity

We briefly recall the numeration objects used to quantify readout space.

Mechanical words and prefix sums. For irrational rotation by α and window offset β, the Sturmian prefix sum identity

$$S_N = \sum_{k=0}^{N-1} s_k = \lfloor N\alpha + \beta \rfloor - \lfloor \beta \rfloor \tag{80}$$

connects symbolic readout to a rigid "staircase vs line" geometry. This is the basic tool for translating prefix length into approximation/resolution.

Ostrowski numeration. Let $\alpha \in (0,1)$ have continued fraction expansion $\alpha = [0; a_1, a_2, \dots]$ and convergents p_n/q_n. Ostrowski numeration represents integers as constrained digit sums over the denominators q_n. The digit constraints are determined by the partial quotients a_n; see standard references in Diophantine approximation [6, 7].

Golden specialization. For $\alpha = \varphi^{-1}$ one has $a_n \equiv 1$ and $q_n = F_{n+1}$ (Fibonacci numbers). The digit constraints reduce to "no adjacent 1" in a Fibonacci basis, yielding Zeckendorf uniqueness [5].

Space complexity meaning. In the scan–readout semantics, the Ostrowski/Zeckendorf digit length is a discrete measure of how much orthogonal-cut grammar is needed to specify the readout coordinate at a given resolution.

D Oracle language and interactive observers

This appendix clarifies the formal position of the oracle/interaction vocabulary used in Section 7.4.

D.1 Oracle (relative computability)

An oracle machine (o-machine) extends a Turing machine with access to an external predicate that can be queried but not computed internally [25]. In modern complexity language, this is the basis of relativization and oracle complexity classes.

In this paper, "oracle-like" is used as a resource-language label: when a readout/selection step conditions on a predicate that is undecidable from within the model, one may consistently describe the conditioning as supplying an external resource.

D.2 Interaction (process vs function)

Observation is modeled as an ongoing process rather than a one-shot input–output function. This motivates using interactive computation language, where the environment is a stream and the observer is an online machine. The analogy to interactive proof systems is especially useful as a resource metaphor: interaction can raise verification power, culminating in the theorem IP = PSPACE [33].

D.3 What is not claimed

Nothing in this paper claims that physical reality literally contains oracle hardware. The oracle/interaction vocabulary is explicitly placed in the interpretation/interface layer, as a way to talk about conditionalization and resource accounting while keeping theorem-level statements (unitarity, locality, undecidability) logically separate.

E Quantitative readout bounds: discrepancy, resolution, and digit depth

This appendix turns several qualitative readout claims into quantitative statements that can be cited or verified directly.

E.1 A sharp discrepancy identity for mechanical words

Let $\alpha \in (0,1) \setminus \mathbb{Q}$ and let $\beta \in \mathbb{R}$. Define the mechanical word

$$s_k := \lfloor (k+1)\alpha + \beta \rfloor - \lfloor k\alpha + \beta \rfloor \in \{0,1\}. \tag{81}$$

Then the prefix sum satisfies the exact identity

$$S_N := \sum_{k=0}^{N-1} s_k = \lfloor N\alpha + \beta \rfloor - \lfloor \beta \rfloor. \tag{82}$$

This is equivalent to Equation (7) after fixing the window convention.

Proposition E.1 (Uniform discrepancy bound)**.** *For all $N \geq 1$,*

$$\left| S_N - N\alpha \right| < 1. \tag{83}$$

Consequently,

$$\left| \frac{S_N}{N} - \alpha \right| < \frac{1}{N}. \tag{84}$$

Proof. Write $S_N = \lfloor N\alpha + \beta \rfloor - \lfloor \beta \rfloor$. Then $S_N \leq N\alpha + \beta - \lfloor \beta \rfloor < S_N + 1$. Subtract $N\alpha$ and note $\beta - \lfloor \beta \rfloor \in [0,1)$. □

Corollary E.2 (Prefix length for relative accuracy)**.** *If a readout task reduces to estimating α by S_N/N and one requires error $\leq \epsilon$, it suffices to take*

$$N \geq \left\lceil \frac{1}{\epsilon} \right\rceil. \tag{85}$$

This is the simplest quantitative instance of Definition 3.3: in the Sturmian scan model, readout resolution improves at least as $O(1/N)$.

E.2 Denjoy–Koksma control at continued-fraction times

Let $\alpha = [0; a_1, a_2, \dots]$ and let p_n/q_n be its convergents. Denjoy–Koksma type inequalities bound Birkhoff sums of bounded-variation functions along the rotation by α at times q_n; see standard discrepancy references [7].

Theorem E.3 (Denjoy–Koksma inequality for rotations (quoted))**.** *Let $f : S^1 \to \mathbb{R}$ have bounded variation $\mathrm{Var}(f)$. For irrational rotation $T(x) = x + \alpha$ and convergent denominators q_n,*

$$\left| \sum_{k=0}^{q_n - 1} f(T^k x) - q_n \int_{S^1} f \, d\mu \right| \leq \mathrm{Var}(f) \tag{86}$$

for all x.

Specializing f to the indicator of an interval (a window), $\mathrm{Var}(f) = 2$, so the deviation of the window-hit count from its mean is uniformly bounded at the convergent times. This yields a rigorous notion of "stability scales" tied to continued fractions.

E.3 Golden anti-resonance as a quantitative extremum

The golden ratio φ is extremal for rational approximation. Hurwitz's theorem implies that every irrational α has infinitely many rationals p/q with $|\alpha - p/q| < 1/(\sqrt{5}q^2)$, and the constant $1/\sqrt{5}$ is optimal. Moreover, for $\alpha = \varphi^{-1}$ one has the lower bound

$$\left|\varphi^{-1} - \frac{p}{q}\right| \geq \frac{1}{\sqrt{5}\,q^2} \qquad \text{for all } \frac{p}{q} \in \mathbb{Q}. \tag{87}$$

See, for example, [6, Ch. II].

This quantifies the "anti-resonance" claim: the golden scan minimizes the possibility of short rational lock-in at a given denominator budget.

E.4 Digit depth scaling in the golden branch

In the golden branch, convergent denominators are Fibonacci numbers, $q_n = F_{n+1}$. Using Binet's formula one has the standard bounds for $n \geq 2$,

$$\varphi^{n-2} \leq F_n \leq \varphi^{n-1}. \tag{88}$$

Therefore the Zeckendorf digit depth m (the index of the largest Fibonacci number used) satisfies

$$m = \Theta(\log N), \qquad N \sim F_m \sim \frac{\varphi^m}{\sqrt{5}}. \tag{89}$$

Combining this with Corollary E.2, one obtains an explicit resolution-to-digit-depth relation:

Proposition E.4 (Resolution vs digit depth (golden case))**.** *To achieve relative readout error $\leq \epsilon$ via Sturmian prefix statistics, it suffices to take $N \geq \lceil 1/\epsilon \rceil$. In the golden branch, the corresponding Zeckendorf digit depth obeys*

$$m \geq \log_\varphi\left(\sqrt{5}\,\epsilon^{-1}\right) + O(1). \tag{90}$$

Thus $S_{\mathrm{read}}(\epsilon) = \Theta(\epsilon^{-1})$ while $S_{\mathrm{code}} = \Theta(\log(\epsilon^{-1}))$.

These relations make the "space as resolution" claim quantitative and highlight a dual notion of space: raw prefix length (a streaming memory cost) versus canonical digit depth (a compressed description length).

E.5 Stability under imperfect readout: a bit-flip noise model

The bounds above are deterministic statements about the underlying mechanical word $s_k \in \{0, 1\}$. To connect to realistic readout, it is useful to quantify how the required prefix length changes under a minimal noise model.

Noise model. Assume the observed bits are corrupted by independent bit-flips:

$$\widetilde{s}_k := s_k \oplus \xi_k, \qquad \xi_k \sim \mathrm{Bernoulli}(p), \qquad 0 \leq p < \tfrac{1}{2}, \tag{91}$$

independently over k. Let $S_N = \sum_{k=0}^{N-1} s_k$ and $\widetilde{S}_N = \sum_{k=0}^{N-1} \widetilde{s}_k$. Then

$$\mathbb{E}[\widetilde{S}_N] = (1 - 2p)\, S_N + pN. \tag{92}$$

If p is known (or separately calibrated), a natural unbiased estimator of S_N is

$$\widehat{S}_N := \frac{\widetilde{S}_N - pN}{1 - 2p}, \qquad \widehat{\alpha}_N := \frac{\widehat{S}_N}{N}. \tag{93}$$

Proposition E.5 (High-probability accuracy under bit-flip noise)**.** *Fix $\delta \in (0,1)$. Under the model above, for all $N \geq 1$,*

$$\mathbb{P}\left(|\widehat{\alpha}_N - \alpha| \;\leq\; \frac{1}{N} + \frac{1}{1-2p}\sqrt{\frac{\log(2/\delta)}{2N}} \right) \;\geq\; 1-\delta. \tag{94}$$

Consequently, to ensure $|\widehat{\alpha}_N - \alpha| \leq \epsilon$ with probability at least $1-\delta$, it suffices to take

$$N \;\geq\; \max\left\{ \left\lceil \epsilon^{-1} \right\rceil,\; \left\lceil \frac{\log(2/\delta)}{2(1-2p)^2\,(\epsilon - 1/N)^2} \right\rceil \right\}, \tag{95}$$

and in the noise-dominated regime one has the scaling $N = \Theta\big((1-2p)^{-2}\epsilon^{-2}\log(1/\delta)\big)$.

Proof. Decompose

$$\widehat{\alpha}_N - \alpha \;=\; \left(\frac{S_N}{N} - \alpha\right) \;+\; \frac{1}{N(1-2p)}\left(\widetilde{S}_N - \mathbb{E}[\widetilde{S}_N]\right). \tag{96}$$

The deterministic discrepancy bound gives $|S_N/N - \alpha| < 1/N$ (Proposition E.1). Conditional on $\{s_k\}$, the random variables $\widetilde{s}_k - \mathbb{E}[\widetilde{s}_k]$ are independent and lie in $[-1,1]$. Hoeffding's inequality [35] yields

$$\mathbb{P}\left(\left|\widetilde{S}_N - \mathbb{E}[\widetilde{S}_N]\right| \;\leq\; \sqrt{\frac{N\log(2/\delta)}{2}} \right) \;\geq\; 1-\delta. \tag{97}$$

Divide by $N(1-2p)$ and combine with the deterministic term to obtain (94). □

Remark E.6 (Interpretation for readout space complexity)**.** *Proposition E.5 cleanly separates two contributions: the intrinsic $O(1/N)$ deterministic discrepancy term from the rotation coding, and a stochastic $O(N^{-1/2})$ term induced by measurement noise. Thus, for sufficiently small ϵ the noise-dominated regime forces the familiar $N = \Theta(\epsilon^{-2})$ sample-complexity scaling. This is the quantitative sense in which imperfect readout increases the operational space cost of stabilization.*

F Routing overhead and 1D compilation: quantitative bounds

This appendix makes the compilation notion used in Proposition 2.6 quantitatively explicit. The goal is not to re-prove all compilation technology but to (i) formalize the overhead functional κ and (ii) record standard upper/lower bounds that tie κ to graph geometry.

F.1 A canonical definition of routing overhead

Let $G_R = (V_R, E_R)$ be the interaction graph of a finite region R for a single PQCA step, with $n := |V_R|$. Assume the PQCA step on R can be expressed as a constant-depth circuit of two-site gates along edges of G_R (this is the standard "local finite-depth" meaning of PQCA).

Let L_n be the path graph on n vertices (a 1D nearest-neighbor line). A *layout* is an injection $f : V_R \to \{1,\dots,n\}$ specifying where each site is placed on the line. Given f, let $\mathrm{depth}_{1\mathrm{D}}(U_R; f)$ be the minimal depth of a 1D nearest-neighbor circuit on L_n that implements U_R up to the fixed encoding/decoding isometries of Proposition 2.6.

Definition F.1 (Routing overhead)**.** *Define the routing overhead of the region update as*

$$\kappa(R) := \min_f \;\mathrm{depth}_{1\mathrm{D}}(U_R; f). \tag{98}$$

When comparing to an "ideal" connectivity where the same circuit has constant depth d_0, one may also consider the dimensionless ratio $\kappa(R)/d_0$.

This definition is purely operational: κ is a resource functional determined by locality constraints and implementability.

F.2 Bandwidth as a universal lower bound

For a layout f, define the bandwidth

$$\mathrm{bw}(G_R, f) := \max_{\{u,v\}\in E_R} |f(u) - f(v)|. \tag{99}$$

Intuitively, an edge spanning distance d requires at least $d-1$ nearest-neighbor swaps to bring its endpoints adjacent at some time. This yields a robust lower bound.

Proposition F.2 (Bandwidth lower bound)**.** *For any layout f,*

$$\mathrm{depth}_{1\mathrm{D}}(U_R; f) \geq c\,\mathrm{bw}(G_R, f) \tag{100}$$

for a constant $c > 0$ that depends only on the allowed local gate radius and on whether swaps and interaction gates can be parallelized in the same layer. Consequently,

$$\kappa(R) \;\geq\; c\,\mathrm{bw}(G_R), \qquad \mathrm{bw}(G_R) := \min_f \mathrm{bw}(G_R, f). \tag{101}$$

Rigorous formulations of bandwidth-based lower bounds are standard in VLSI layout and in nearest-neighbor circuit compilation.

Remark F.3 (Explicit constants and interaction range)**.** *If the 1D target architecture allows only nearest-neighbor swaps and two-site gates, and one counts depth in layers of disjoint nearest-neighbor operations, then a qubit can move by at most one site per layer. Hence two qubits separated by distance d can reduce their separation by at most 2 per layer, so making them adjacent requires at least $\lceil (d-1)/2 \rceil$ layers. In this standard accounting one may take $c \geq 1/2$ up to lower-order additive constants.*

Remark F.4 (Dependence on geometric interaction radius)**.** *If a single PQCA step includes two-site interactions within geometric graph distance at most r (a bounded interaction range), then G_R is the corresponding r-neighborhood interaction graph. For fixed $r = O(1)$, the boundary/bandwidth scaling exponents in Theorem F.6 are unchanged; the dependence on r enters only through constants in the $\Omega(\cdot)$ and $O(\cdot)$ bounds.*

F.3 A constructive linear upper bound via swap networks

A matching universal upper bound follows from the existence of depth-$O(n)$ swap networks that realize any permutation of n items on a line. A classical example is odd–even transposition sorting (brick sort), which implements any permutation in depth n using nearest-neighbor swaps [36]. Quantum-circuit formulations of this "compute permutations with adjacent swaps" primitive for linear-nearest-neighbor architectures are discussed, for example, by Kutin–Moulton–Smithline [10].

Proposition F.5 (Universal $O(n)$ 1D compilation bound)**.** *Let U_R be a constant-depth circuit of bounded-degree two-site gates on n sites. Then there exists a 1D nearest-neighbor implementation with*

$$\mathrm{depth}_{1\mathrm{D}}(U_R) = O(n). \tag{102}$$

The constant in $O(n)$ depends only on the maximal degree and on the number of circuit layers in the PQCA step.

Proof. Route, layer by layer, the disjoint pairs of qubits that need to interact. Each layer induces a partial matching on V_R. Use a swap network to permute the line so that each matched pair becomes adjacent; apply all gates in parallel; then undo (or continue with a new permutation for the next layer). Odd–even transposition provides a depth-n permutation primitive. □

This shows that Proposition 2.6 is not merely existential: it has a concrete depth scaling.

F.4 Grid regions: overhead scales like boundary area

For a 2D $L \times L$ grid (the Cartesian product $P_L \times P_L$) with nearest-neighbor interactions, the bandwidth is exactly

$$\mathrm{bw}(P_L \times P_L) = L, \tag{103}$$

as shown by Chvátalová [37]. For higher-dimensional grids, Billera–Blanco give an explicit formula for the bandwidth of P_L^d (the d-fold Cartesian product of a length-L path) and, in particular, show that for fixed d one has the asymptotic scaling

$$\mathrm{bw}(P_L^d) = \Theta(L^{d-1}). \tag{104}$$

See [38] and references therein for related product-graph bandwidth results (see also [39] for classical optimal-numbering/isoperimetric perspectives).

Since the boundary size also scales as $|\partial R| = \Theta(L^{d-1})$, one obtains a geometric law:

Theorem F.6 (Boundary-scaling compilation overhead)**.** *Let R be a d-dimensional cubic grid region of side length L with bounded-range local interactions. Then the minimal 1D nearest-neighbor compilation depth for one local update obeys*

$$\kappa(R) = \Omega(L^{d-1}) = \Omega(|\partial R|), \tag{105}$$

and there exists a compilation with depth $O(n) = O(L^d)$. In particular, for $d = 2$ one has $\kappa(R) = \Omega(L) = \Omega(\sqrt{n})$.

Proof. For a local nearest-neighbor update on a d-dimensional L^d grid region, the interaction graph contains (up to constant-radius thickening) the grid adjacency P_L^d. Therefore its bandwidth is at least that of P_L^d. By Proposition F.2, any 1D nearest-neighbor implementation depth is lower-bounded (up to a locality-dependent constant) by bandwidth, hence $\kappa(R) = \Omega(\mathrm{bw}(P_L^d))$. The scaling $\mathrm{bw}(P_L^d) = \Theta(L^{d-1})$ for fixed d follows from [38] (and for $d = 2$ one has the exact value L by [37]). Since $|\partial R| = \Theta(L^{d-1})$, this yields $\kappa(R) = \Omega(|\partial R|)$. The upper bound $O(n)$ follows from Proposition F.5. □

This theorem gives a quantitatively rigid bridge from geometry to computation: encoding higher-dimensional locality into 1D forces an overhead controlled by a boundary-like measure. Under the lapse definition $N = \kappa_0/\kappa$, this becomes a precise "time slows down where compilation gets expensive" statement.

G Undecidable local reachability in universal QCA: a reduction

This appendix provides a concrete halting-to-reachability reduction establishing Theorem 2.7. Once a fixed local, reversible dynamics can simulate a universal machine and a halting event is recorded in a localized flag, the corresponding hitting predicate is undecidable by a direct reduction from halting. For classical CA undecidability results in closely related settings see, e.g., [23,24]. For undecidability results about reachability properties of quantum-system models (quantum automata), see [40].

G.1 Formal predicate

Fix a lattice $\mathbb{Z}$ and a local Hilbert space $\mathbb{C}^d$ per site. Let U be a QCA update on $\bigotimes_{n\in\mathbb{Z}} \mathbb{C}^d$. For a finite region K and a local projector Π_K supported on K, define the *local reachability predicate*

$$\mathsf{Reach}(U, \Pi_K; \psi) \;:=\; \Big[\exists t \geq 0 :\; \langle\psi|U^{\dagger t}\Pi_K U^t|\psi\rangle > 0\Big]. \tag{106}$$

Theorem 2.7 claims the existence of a fixed (U, Π_K) for which $\mathsf{Reach}(U, \Pi_K; \psi_{M,x})$ is undecidable as a function of the encoded instance (M, x).

G.2 Step 1: reversible halting as a well-posed predicate

The classical halting problem is undecidable [41]. To embed it into a unitary dynamics, it is convenient to work with a reversible (injective) machine model. Reversible simulation of Turing machines is standard in reversible computation [11, 42]. In particular, there exist universal reversible Turing machines whose halting behavior encodes the usual halting problem.

G.3 Step 2: a fixed local, reversible dynamics simulating a universal reversible machine

Let $M_\star$ be a fixed universal reversible Turing machine (URTM). Fix a finite tape alphabet Γ, a finite internal state set Q, and a distinguished halting state $q_{\text{halt}} \in Q$. Encode the URTM configuration into a 1D lattice by using a finite local alphabet that stores: (i) a tape symbol in Γ, (ii) a head marker plus internal state in Q at exactly one site, and (iii) auxiliary registers used to make halting-event recording reversible [11, 42].
One can implement one URTM step by a translation-invariant, finite-radius reversible local rule (equivalently, a reversible cellular automaton on the computational basis). Promoting this reversible basis permutation to a unitary yields a QCA update U which acts as the classical reversible dynamics on basis states. Universal QCA constructions and QCA structure theorems are discussed in [8, 9, 17, 18].

G.4 Step 3: a localized halting flag projector

Given an instance (M, x), construct an initial basis state $|\psi_{M,x}\rangle$ that encodes M and input x in a finite "program/data" region, with blank padding elsewhere. Reserve a dedicated finite region K containing a "flag cell" whose local basis includes states $|0\rangle$ and $|1\rangle$.

Design the simulation so that: (i) if M halts on x, then at the moment of halting the flag cell is set to $|1\rangle$ and remains $|1\rangle$ thereafter (this can be achieved without violating reversibility by recording the halting event in an ancilla and continuing with a reversible idle loop); (ii) if M does not halt, the flag cell remains $|0\rangle$ forever.

Let Π_K be the local projector onto the subspace where the flag cell is in state $|1\rangle$ (tensored with identity on the rest of K). Then

$$\exists t \geq 0 : \ \langle \psi_{M,x} | U^{\dagger t} \Pi_K U^t | \psi_{M,x} \rangle > 0 \tag{107}$$

holds if and only if M halts on x.

Proof. Because the evolution is classical on the computational basis, for each t the state $U^t|\psi_{M,x}\rangle$ is again a basis state. Hence the quantity $\langle \psi_{M,x} | U^{\dagger t} \Pi_K U^t | \psi_{M,x} \rangle$ is in $\{0, 1\}$ and equals 1 iff the flag cell is in state $|1\rangle$ at time t. By construction, the flag is triggered at some time iff the simulated computation halts. □

G.5 Conclusion: undecidability

If there were an algorithm deciding the reachability predicate above for all (M, x), it would decide halting. Therefore the local reachability predicate is undecidable.

Remark G.1 (Why this is compatible with unitarity)**.** *The construction never modifies U nonunitarily. Undecidability arises because the predicate quantifies over unbounded time and because universal dynamics can encode arbitrarily long computations.*

G.6 Robustness: a thresholded reachability predicate

The bare predicate $\exists t : \langle \Pi_K \rangle > 0$ is intentionally sharp, but it is not robust under arbitrary perturbations of the initial encoding: an arbitrarily small component in the flag subspace would make the inequality true. One can, however, state a robust version that remains equivalent for perturbations bounded in trace distance.

Lemma G.2 (Projector expectation is Lipschitz in trace distance)**.** *For any two density operators ρ, σ and any projector Π,*

$$\big|\mathrm{Tr}(\Pi\rho) - \mathrm{Tr}(\Pi\sigma)\big| \;\le\; D(\rho,\sigma), \qquad D(\rho,\sigma) := \tfrac{1}{2}\|\rho-\sigma\|_1. \tag{108}$$

Proof. This is standard: for any effect $0 \le E \le \mathbb{1}$ one has $|\mathrm{Tr}(E(\rho-\sigma))| \le \frac{1}{2}\|\rho-\sigma\|_1$; see, e.g., [3]. □

Proposition G.3 (Robust halting-to-reachability with a probability threshold)**.** *Let U and Π_K be as in the reduction above and let $\rho_{M,x} := |\psi_{M,x}\rangle\langle\psi_{M,x}|$ be the ideal basis-state encoding. Assume the reduction is* deterministic on the computational basis *so that for all t,*

$$\mathrm{Tr}\big(\Pi_K\, U^t \rho_{M,x} U^{\dagger t}\big) \in \{0,1\}, \tag{109}$$

and there exists a time $t_\star$ such that this quantity equals 1 if and only if M halts on x. Let $\widetilde{\rho}$ be an imperfect encoding with $D(\widetilde{\rho}, \rho_{M,x}) \le \delta$. Then for every t,

$$\big|\mathrm{Tr}(\Pi_K\, U^t \widetilde{\rho} U^{\dagger t}) - \mathrm{Tr}(\Pi_K\, U^t \rho_{M,x} U^{\dagger t})\big| \;\le\; \delta, \tag{110}$$

and in particular, if $\delta < 1/2$ the thresholded predicate

$$\exists t \ge 0 :\; \mathrm{Tr}(\Pi_K\, U^t \widetilde{\rho} U^{\dagger t}) \;\ge\; 1/2 \tag{111}$$

is true if and only if M halts on x.

Proof. Unitary evolution preserves trace distance: $D(U^t\widetilde{\rho}U^{\dagger t}, U^t\rho_{M,x}U^{\dagger t}) = D(\widetilde{\rho}, \rho_{M,x})$. Apply Lemma G.2. If M does not halt then the ideal expectation is 0 for all t, hence the imperfect expectation is $< 1/2$ for all t. If M halts then at $t = t_\star$ the ideal expectation is 1, hence the imperfect expectation is $> 1/2$. □

H From routing overhead to a relativistic lapse: an axiomatic correspondence

This appendix records an explicit mapping under which the computational lapse $\mathcal{N}(x) = \kappa_0/\kappa(x)$ reproduces the kinematic role of a relativistic lapse function. The goal is to make the correspondence operational and quantitatively checkable under explicit axioms relating geometry to compilation overhead.

H.1 A minimal operational statement

Fix a baseline depth time t measured in 1D nearest-neighbor circuit depth. By definition, the local logical time τ_{loc} counts locally realizable logical steps. If implementing one logical step at location x requires routing overhead $\kappa(x)$ (Definition F.1), then

$$d\tau_{\mathrm{loc}}(x) = \frac{\kappa_0}{\kappa(x)}\, dt \;=\; \mathcal{N}(x)\, dt, \tag{112}$$

which is Equation (12).

H.2 A geometry-to-κ model via boundary scaling

To connect κ to geometric data, one must specify how a spatial region and its local interaction structure are encoded into an interaction graph. We formalize this as a geometric rigidity postulate.

Axiom H.1 (Geometric rigidity of overhead)**.** *At each location x, the effective local update acts on a region $R(x)$ whose interaction graph contains a d-dimensional cubic grid of side length $L(x)$ at bounded interaction range, and the minimal 1D compilation depth saturates the boundary-scaling lower bound up to a fixed constant factor:*

$$\kappa(x) = c\, L(x)^{d-1}, \tag{113}$$

for some constant $c > 0$ independent of x.

By Theorem F.6, the scaling $\kappa(x) = \Omega(L(x)^{d-1})$ is unavoidable under 1D embedding; Axiom H.1 asserts that the realized compilation is asymptotically optimal in this sense. Under Axiom H.1, the lapse scales as

$$\mathcal{N}(x) \;=\; \frac{\kappa_0}{c}\, L(x)^{-(d-1)}. \tag{114}$$

H.3 Relativistic kinematics: redshift from κ

For a static spacetime metric in ADM form,

$$ds^2 = -N(x)^2\, dt^2 + h_{ij}(x)\, dx^i dx^j, \tag{115}$$

proper time obeys $d\tau = N(x)\, dt$ for observers at rest in the chosen coordinates. Define the emergent lapse by

$$N(x) := \mathcal{N}(x) = \frac{\kappa_0}{\kappa(x)}. \tag{116}$$

Then the gravitational redshift factor between two static observers at x_{em} and x_{obs} is

$$\frac{\nu_{\mathrm{obs}}}{\nu_{\mathrm{em}}} = \frac{N(x_{\mathrm{obs}})}{N(x_{\mathrm{em}})} = \frac{\kappa(x_{\mathrm{em}})}{\kappa(x_{\mathrm{obs}})}, \tag{117}$$

so frequency shifts become directly measurable ratios of compilation overheads.

H.4 Matching a target relativistic lapse (example)

Consider a static spacetime metric in ADM form

$$ds^2 = -N(x)^2\, dt^2 + h_{ij}(x)\, dx^i dx^j, \tag{118}$$

so that proper time obeys $d\tau = N(x)\, dt$ for observers at rest in the chosen coordinates. Given a target lapse profile $N(x)$, the boundary-scaling model (114) suggests choosing a geometric scale field $L(x)$ such that

$$L(x) \;\propto\; N(x)^{-1/(d-1)}. \tag{119}$$

For instance, in $d = 2$ one has $L(x) \propto N(x)^{-1}$. In particular, for a Schwarzschild-like kinematic lapse $N(r) = \sqrt{1 - 2GM/r}$ (in units $c = 1$), the corresponding overhead profile is

$$\kappa(r) \;\propto\; \frac{1}{\sqrt{1 - 2GM/r}}, \tag{120}$$

which makes the "clock rate" slowdown an explicit routing/compilation slowdown.

References

[1] Marston Morse and Gustav A. Hedlund. Symbolic dynamics II. Sturmian trajectories. *American Journal of Mathematics*, 62(1):1–42, 1940.

[2] M. Lothaire. *Algebraic Combinatorics on Words*. Cambridge University Press, Cambridge, 2002.

[3] John Watrous. *The Theory of Quantum Information*. Cambridge University Press, Cambridge, 2018.

[4] Michael A. Nielsen and Isaac L. Chuang. *Quantum Computation and Quantum Information*. Cambridge University Press, 2012.

[5] E. Zeckendorf. Représentation des nombres naturels par une somme de nombres de Fibonacci ou de nombres de Lucas. *Bulletin de la Société Royale des Sciences de Liège*, 41:179–182, 1972.

[6] J. W. S. Cassels. *An Introduction to Diophantine Approximation*. Cambridge University Press, Cambridge, 1957.

[7] L. Kuipers and Harald Niederreiter. *Uniform Distribution of Sequences*. Wiley, New York, 1974.

[8] Benjamin Schumacher and Reinhard F. Werner. Reversible quantum cellular automata. *arXiv preprint arXiv:quant-ph/0405174*, 2004.

[9] Pablo Arrighi, Vincent Nesme, and Reinhard Werner. Unitarity plus causality implies localizability. *Journal of Computer and System Sciences*, 77(2):372–378, 2011.

[10] Samuel A. Kutin, David Petrie Moulton, and Lawren M. Smithline. Computation at a distance. *arXiv preprint arXiv:quant-ph/0701194*, 2007.

[11] Charles H. Bennett. Time/space trade-offs for reversible computation. *SIAM Journal on Computing*, 18(4):766–776, 1989.

[12] Marc A. Rieffel. C*-algebras associated with irrational rotations. *Pacific Journal of Mathematics*, 93(2):415–429, 1981.

[13] Serge Massar and Philippe Spindel. Uncertainty relation for the discrete fourier transform. *Physical Review Letters*, 100(19):190401, 2008.

[14] P. Carruthers and Michael Martin Nieto. Phase and angle variables in quantum mechanics. *Reviews of Modern Physics*, 40(2):411–440, 1968.

[15] D. T. Pegg and S. M. Barnett. Phase properties of the quantized single-mode electromagnetic field. *Physical Review A*, 39(4):1665–1675, 1989.

[16] Elliott H. Lieb and Derek W. Robinson. The finite group velocity of quantum spin systems. *Communications in Mathematical Physics*, 28(3):251–257, 1972.

[17] John Watrous. On one-dimensional quantum cellular automata. In *Proceedings of the 36th Annual Symposium on Foundations of Computer Science (FOCS)*, pages 528–537. IEEE, 1995.

[18] Pablo Arrighi and Jonathan Grattage. Intrinsically universal n-dimensional quantum cellular automata. *arXiv preprint arXiv:0907.3827*, 2010.

[19] Iwo Bialynicki-Birula. Weyl, dirac, and maxwell equations on a lattice as unitary cellular automata. *Physical Review D*, 49(12):6920–6927, 1994.

[20] Pablo Arrighi, Vincent Nesme, and Marcelo Forets. The dirac equation as a quantum walk: higher dimensions, observational convergence. *Journal of Physics A: Mathematical and Theoretical*, 47(46):465302, 2014.

[21] Pablo Arrighi, Giuseppe Di Molfetta, Iván Márquez-Martín, and Armando Pérez. Dirac equation as a quantum walk over the honeycomb and triangular lattices. *Physical Review A*, 97(6):062111, 2018.

[22] H. B. Nielsen and M. Ninomiya. A no-go theorem for regularizing chiral fermions. *Physics Letters B*, 105(2-3):219–223, 1981.

[23] Jarkko Kari. Reversibility of 2d cellular automata is undecidable. *Physica D: Nonlinear Phenomena*, 45(1-3):379–385, 1990.

[24] Jarkko Kari. Reversibility and surjectivity problems of cellular automata. *Journal of Computer and System Sciences*, 48(1):149–182, 1994.

[25] A. M. Turing. Systems of logic based on ordinals. *Proceedings of the London Mathematical Society*, 45(1):161–228, 1939.

[26] Peter Wegner. Why interaction is more powerful than algorithms. *Communications of the ACM*, 40(5):80–91, 1997.

[27] Uri Jacob and Tsvi Piran. Lorentz-violation-induced arrival delays of cosmological particles. *Journal of Cosmology and Astroparticle Physics*, 2008(01):031, 2008.

[28] V. Vasileiou, A. Jacholkowska, F. Piron, J. Bolmont, J. Granot, F. W. Stecker, J. Cohen-Tanugi, and F. Longo. Constraints on lorentz invariance violation from Fermi-Large Area Telescope observations of gamma-ray bursts. *Physical Review D*, 87:122001, 2013.

[29] A. A. Abdo et al. A limit on the variation of the speed of light arising from quantum gravity effects. *Nature*, 462:331–334, 2009.

[30] David Mattingly. Modern tests of lorentz invariance. *Living Reviews in Relativity*, 8(1):5, 2005.

[31] Holger Müller, Sven Herrmann, Alejandro Saenz, Achim Peters, and Claus Lämmerzahl. Optical cavity tests of lorentz invariance for the electron. *Physical Review D*, 68(11):116006, 2003.

[32] Shafi Goldwasser, Silvio Micali, and Charles Rackoff. The knowledge complexity of interactive proof systems. *SIAM Journal on Computing*, 18(1):186–208, 1989.

[33] Adi Shamir. Ip = pspace. *Journal of the ACM*, 39(4):869–877, 1992.

[34] Carl W. Helstrom. *Quantum Detection and Estimation Theory.* Academic Press, New York, 1976.

[35] Wassily Hoeffding. Probability inequalities for sums of bounded random variables. *Journal of the American Statistical Association*, 58(301):13–30, 1963.

[36] Donald E. Knuth. *The Art of Computer Programming, Volume 3: Sorting and Searching.* Addison-Wesley, Reading, MA, 2 edition, 1998.

[37] Jarmila Chvátalová. Optimal labelling of a product of two paths. *Discrete Mathematics*, 11(3):249–253, 1975.

[38] Louis J. Billera and Saúl A. Blanco. Bandwidth of the product of paths of the same length. *Discrete Applied Mathematics*, 161(18):3080–3086, 2013.

[39] L. H. Harper. Optimal numberings and isoperimetric problems on graphs. *Journal of Combinatorial Theory*, 1(3):385–393, 1966.

[40] Yangjia Li and Mingsheng Ying. (un)decidable problems about reachability of quantum systems. In *CONCUR 2014 – Concurrency Theory*, volume 8704 of *Lecture Notes in Computer Science*, pages 482–496. Springer, 2014.

[41] A. M. Turing. On computable numbers, with an application to the entscheidungsproblem. *Proceedings of the London Mathematical Society*, 42(2):230–265, 1936.

[42] Charles H. Bennett. Logical reversibility of computation. *IBM Journal of Research and Development*, 17(6):525–532, 1973.